Diplomarbeit

Effect of $TiAl_6V_4$ surface modifications on the expression of matrix metalloproteinases and their inhibitors.

eingereicht von

Sylvester Martin Gabalier

zur Erlangung des akademischen Grades

Doktor der gesamten Heilkunde

(Dr. med. univ.)

an der

Medizinischen Universität Graz

ausgeführt an der

Universitätsklinik für Orthopädie und Traumatologie

unter der Anleitung von

Priv.-Doz. Mag. Dr. scient. med. Birgit Lohberger
und
Priv.-Doz. Dr. med. univ. et scient. med. Patrick Sadoghi

Graz, 05.11.2020

Eidesstattliche Erklärung

Ich erkläre ehrenwörtlich, dass ich die vorliegende Arbeit selbstständig und ohne fremde Hilfe verfasst habe, andere als die angegebenen Quellen nicht verwendet habe und die den benutzten Quellen wörtlich oder inhaltlich entnommenen Stellen als solche kenntlich gemacht habe.

Graz, am 05.11.2020 *Sylvester Martin Gabalier eh.*

Danksagung

Ich möchte mich auf diesem Wege bei Frau Priv.-Doz. Mag. Dr. Birgit Lohberger, sowie ihrem Team, insbesondere Herrn Dietmar Glänzer, MSc und Frau Nicole Eck, MSc, für die grtoßartige Unterstützung, die hilfreichen Arbeitsanweisungen und die sehr lehrreichen und spannenden Stunden, welche ich im Forschungslabor der Universitätsklinik für Orthopädie und Traumatologie verbringen durfte, bedanken.

Table of contents

Abbreviations and their explanations

Ag	. . .	silver
BGLAP	. . .	Osteocalcin
B2M	. . .	Beta-2-microglobulin
cDNA	. . .	complementary deoxyribonucleic acid
CO_2	. . .	carbon dioxide
CoCrMo	. . .	Cobalt-Chrome-Molybdenum alloy
COL1	. . .	collagen type 1
cpTi	. . .	commercially pure titanium
DNA	. . .	deoxyribonucleic acid
ECM	. . .	extracellular matrix
EDX	. . .	energy dispersive x-ray spectroscopy
FBS	. . .	foetal bovine serum
hFOB	. . .	human fetal osteoblasts
IL	. . .	interleucin
kV	. . .	kilovolt
LDH	. . .	lactate dehydrogenase
men	. . .	mean value
µg	. . .	microgramm
min	. . .	minutes
µl	. . .	microliter
mL	. . .	milliliters
MMP	. . .	matrix metalloproteinase
NC	. . .	negative control
NFW	. . .	nuclease free water

nm	. . .	nanometers
NTC	. . .	no template control
PCR	. . .	polymerase chain reaction
PEEK	. . .	polyetheretherketone
RECK	. . .	membrane-anchored inhibitor of MMPs
RPL	. . .	Ribosomal protein
RNA	. . .	ribonucleic acid
RT	. . .	reverse transcriptase
RT-qPCR	. . .	Real-time PCR
SD	. . .	standard deviation
SEM	. . .	scanning electron microscopy
SPP	. . .	Osteopontin
SYBR Green	. . .	fluorescent dye that binds double stranded DNA molecules
THA	. . .	total hip arthroplasty
Ti	. . .	titanium
$TiAl_6V_4$	. . .	metal alloy consisting of: titanium, 6% aluminum and 4% vanadium
TIMP	. . .	tissue inhibitor
TiN	. . .	titanium-nitride
TKA	. . .	total knee arthroplasty
TNF	. . .	tumor necrosis factor

List of figures

Table directory

Zusammenfassung

Zu den Ursachen für die aseptische Lockerung von implantierten Prothesen in der orthopädischen Chirurgie, welche einen häufigen Grund für deren Versagen darstellt, werden nicht nur inadäquate initiale Fixierung der jeweiligen Implantate oder eine, im Laufe der Zeit zunehmende, mechanische Lockerung derselben, sondern auch eine, in der unmittelbaren knöchernen Umgebung des Implantates zu beobachtende, Osteolyse gezählt. Man geht derzeit davon aus, dass als Ursache für diese Osteolyse im periprothetischen Bereich sowohl Partikel, welche durch den mechanischen Abrieb des Prothesenmaterials entstehen, als auch Metallionen, die auf elektrochemischen Wege gelöst werden, anzusehen sind. Unserer Hypothese zufolge wird die Exprimierung von Genen, deren Produkte für die Erneuerung der Extrazellulärmatrix des Knochengewebes und somit für die Aufrechterhaltung ihrer mechanischen Funktion von essenzieller Bedeutung sind, in Osteoblasten verändert, wenn die betreffenden Zellen in direktem Kontakt mit $TiAl_6V_4$-Implantaten, deren Oberflächen unterschiedlich modifiziert sind ($TiAl_6V_4$+TiN, $TiAl_6V_4$+Ag, $TiAl_6V_4$-aufgerauht und $TiAl_6V_4$+cpTi), stehen, was zum Prozess der aseptischen Prothesenlockerung beitragen könnte. Aus diesem Grunde untersuchten wir sowohl die Wirkung, die modifizierte Oberflächen von $TiAl_6V_4$ auf die Genexpression von Matrixmetalloproteinasen (MMP2, MMP9, MMP14) und deren Inhibitoren (TIMP1, TIMP2) sowie von Collagen Typ I (COL1), Osteopontin (SPP) und Osteocalcin (BGLAP) haben, als auch das Ausmaß der Zytotoxizität bei Osteoblasten (hFOB), die auf solchen Oberflächen wachsen. Unsere Untersuchungen zeigten, im Vergleich zu Oberflächen bestehend aus unverändertem $TiAl_6V_4$, keine signifikante Erhöhung der Zytotoxizität bei den oben genannten modifizierten Oberflächen.

Des Weiteren ließ sich feststellen, dass die Genexpression von MMP9 und MMP14 generell sehr niedrig war und, abgesehen von der Gruppe $TiAl_6V_4$+Ag, im Vergleich zu $TiAl_6V_4$ keine signifikanten Unterschiede bei der Exprimierung von MMP2, TIMP1, TIMP2, COL1, SPP oder BGLAP durch hFOB Zellen, die auf den, von uns untersuchten, modifizierten Oberflächen von $TiAl_6V_4$ ($TiAl_6V_4$+TiN, $TiAl_6V_4$-roughening und $TiAl_6V_4$+cpTi) wuchsen, beobachtet werden konnten. Daraus lässt sich schließen, dass die oben genannten Oberflächenmodifikationen keinen wesentlichen Einfluss auf die Expression von MMP2, TIMP1, TIMP2,

COL1, SPP oder BGLAP durch Osteoblasten haben und somit nicht, oder zumindest nicht auf diesem Wege, zu aseptischer Prothesenlockerung und in weiterer Folge dem Versagen von Implantaten beitragen. Die genaue Ursache der, verglichen mit der Gruppe $TiAl_6V_4$, signifikant veränderten Exprimierung von MMP2, TIMP1 und SPP in hFOB-Zellen, welche auf $TiAl_6V_4$+Ag wuchsen und ob zwischen diesen Veränderungen in der Exprimierung jener Gene ein Zusammenhang besteht, konnte in der vorliegenden Diplomarbeit nicht geklärt werden und bedarf weiterer Untersuchungen.

Abstract

Aseptic loosening of implanted prostheses in orthopedic surgery, which is a frequent reason for their failure, is not only attributed to inadequate initial fixation or mechanical loss of fixation over time, but also to osteolysis observed in the surrounding bone. It is currently assumed that this osteolysis in the area surrounding implants is caused both by particles produced by means of mechanical abrasion of the prosthesis material and by metal ions dissolved by electrochemical processes. According to our hypothesis, the expression of genes whose products are essential for the renewal of the extracellular matrix of bone tissue and thus for the maintenance of its mechanical function is altered in osteoblasts if these cells are in direct contact with $TiAl_6V_4$-Implants, whose surfaces have been modified in different ways ($TiAl_6V_4$+TiN, $TiAl_6V_4$+Ag, $TiAl_6V_4$-roughening and $TiAl_6V_4$+cpTi). This could possibly contribute to aseptic prosthesis loosening. Therefore we analysed the impact of this $TiAl_6V_4$ surface modifications on both cytotoxicity and gene expression of matrix metalloproteinases (MMP2, MMP9, MMP14) and their inhibitors (TIMP1, TIMP2) as well as the expression of Collagen type I (COL1), Osteopontin (SPP) and Osteocalcin (BGLAP) in osteoblasts (hFOB). Compared to $TiAl_6V_4$, our investigations did not show any significant increase in cytotoxicity for the modified surfaces we investigated. Furthermore, it has been found that the gene expression of MMP9 and MMP14 was generally very low, and with the exception of the group $TiAl_6V_4$+Ag no significant differences in the expression of MMP2, TIMP1, TIMP2, COL1, SPP or BGLAP by hFOB cells growing on the modificated surfaces of $TiAl_6V_4$ we investigated ($TiAl_6V_4$+TiN, $TiAl_6V_4$-roughening and $TiAl_6V_4$+cpTi) could be found compared to $TiAl_6V_4$. From that it can be concluded that the above mentioned surface modifications do not have any significant influence on the expression of MMP2, TIMP1, TIMP2, COL1, SPP or BGLAP by osteoblasts and thus do not, or at least not by this pathway, contribute to aseptic prosthesis loosening. The cause of the significantly different expression of MMP2, TIMP1 and SPP in hFOB cells growing on $TiAl_6V_4$+Ag compared to the group $TiAl_6V_4$ and whether or not there is a relationship between these changes in the expression of those genes could not be clarified in the present diploma thesis and will require further investigations.

1 Introduction

1.1 Titanium Based Alloys

Biomaterials are substances that have been engineered to take a form which, alone or as part of a complex system, is used to direct, by control of interactions with components of living systems, the course of any therapeutic or diagnostic procedure, in human or veterinary medicine [1] but they could also be defined as systematically, pharmacologically inert substances designed for implantation within or in corporation with living systems. [2,3] Biomaterials can be divided into five major classes: metals and their alloys, polymers, ceramics, composites and natural materials, [4,5] whereby among the metals, stainless steel, cobalt chromium alloys, and titanium based alloys are the most commonly used in various orthopaedic applications like fracture fixation or total joint replacement. [6,7] Titanium and titanium based alloys have been used as implant materials since the 1960‘s. [8] They display better biocompatibility than stainless steel and cobalt based alloys, excellent corrosion resistance, fatigue strength and light weight and have therefore emerged as the number one choice for orthopaedic implant materials. [9-12] $TiAl_6V_4$ (titanium; 6% aluminum; 4% vanadium) occupies the most important position among all the Ti alloys. [13]

Titanium:
has excellent mechanical properties and biocompatibility for clinical use under load-bearing conditions. [14]

Aluminum:
is able to increase the strength of the alloy and decrease its density. [15,16]

Vanadium:
Improves the alloys ductiliy. [15]

1.2 The Benefit of Surface Modifications

To improve the bone anchorage and bioactivity of titanium based alloys different types of surface modification techniques have been used. [11,17-20] These modification techniques can be divided into three categories depending on the characteristics brought on the surface: physical (eg. Grit blasting, Laser treatment, Machining, Plasma spraying), chemical (eg. Acid etching, Alkali treatment, Anodic oxidation), and biological (eg. Biological coatings). [13] For our experiments we used $TiAl_6V_4$ metal alloys with the following surfaces/surface modifications:

$TiAl_6V_4$+TiN:

Titanium-nitride (TiN) is a ceramic with great hardness that is used for coatings because of its positive effect on the biocompatibility and tribological properties of implant surfaces. [21] TiN coatings have shown a high level of wear resistance to in vivo loading. [22]

$TiAl_6V_4$+Ag:

Silver coatings of titanium implants are used because of their high antibacterial efficacy combined with low toxicity to eukaryotic cells. [23,24]

$TiAl_6V_4$ roughening:

Surfaces of implants are roughened to enhance differentiation and attachment of bone cells, and increase mineralization. [25,26]

$TiAl_6V_4$+cpTi:

Commercially pure (cp)-Ti surfaces of implants provide stable fixation, and good biocompatibility. [11] Shah et al. found, that cp-Ti and $TiAl_6V_4$ demonstrate similar osseointegration and biomechanical anchorage. [27]

1.3 Osseointegration

An implant is considered as osseointegrated when there is no progressive relative movement between the implant and the surface of the bone with which it is in direct contact. [5,25,28] Important stages of the osseointegration process are blood clot formation and mesenchymal tissue development, its replacement with woven bone, and, finally, lamellar bone formation replacing the woven bone. [5,28]

1.4 Aseptic Prosthesis Loosening

A major cause of implant failure in orthopaedic surgery is aseptic loosening. [29-35] Schwartz et al. reported that for total revision of knee arthroplasty (TKA), infection and aseptic loosening were the two most common modes of failure in the United States between 2002 and 2014 according to data obtained from the national inpatient sample database. [29] Halvorsen et al. analyzed the outcome of patients 21 years or younger with total hip arthroplasties (THAs). They included all THA patients 21 years or younger reported during 1995 through 2016 to the Danish, Finnish, Norwegian, and Swedish hip arthroplasty registers and found that aseptic loosening was the main cause of revision. [30]

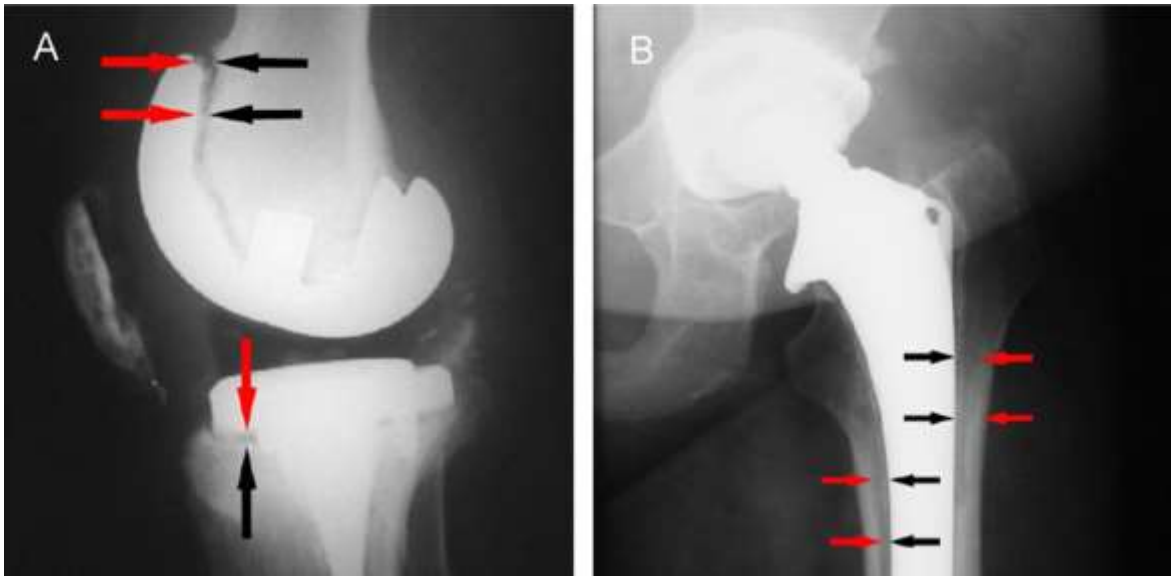

Figure 1:
Radiological appearance of a total knee endoprosthesis (A) and a total hip endoprosthesis (B) with a zone of periprosthetic whitening of more than 2 mm (between the arrows), indicating a septic or an aseptic prosthesis loosening [36].

Aseptic loosening can be the result of inadequate initial fixation, mechanical loss of fixation over time, or biologic loss of fixation caused by particle induced osteolysis around the implant. [32] The degradation products of an orthopaedic implant not only include particles produced by mechanical wear that are phagocytosable and have the potential to elicit an inflammatory response [37] but also soluble deposits (metal ions) caused by electrochemical dissolution. [35,38,39] Titanium based alloys used for orthopaedic appliances rely on the formation of a passive film consisting of metal oxides, which forms spontaneously on the surface of the metal, to prevent oxidation from taking place. [38] This film has been proposed as a two-layer oxide:

1) an inner layer, mainly composed by TiO_2 responsible for the high corrosion resistance of the passive film and

2) a porous layer, with lower corrosion resistance, composed by TiO_2 and enriched with aluminum (Al_2O_3) and vanadium (V_2O_5) oxides. [40]

If mechanical factors damage the oxide film, ions could be released into solution. The release of metallic particles and/or ions is commonly associated with inflammatory responses and the activation of osteoclasts, which may lead to bone resorption and, ultimately, the implant loosening. [5,32,34,35,40-42]

1.5 Bone Extracellular Matrix

The extracellular matrix (ECM) of bones consists of hydroxyapatite, a variant of calcium phosphate which, together with some water, crystallizes in a matrix of collagen and some other organic materials like non-collagenous glycoproteins, hyaluronan and proteoglycans. [43,44] Proteins and signalling pathways that influence the mineral or organic components of bone ECM, or regulate bone remodelling by osteoblasts (responsible for bone formation), osteoclasts (responsible for bone resorption) and osteocytes, affect the material properties and thus the quality of bone ECM. [45] It has been shown that particulate debris influences both the cytokine release of human osteoblasts, which could lead to

increased degeneration of the bone matrix through the cytokine-induced differentiation of osteoclasts for matrix degradation, and inhibits the regeneration of the bone matrix through the reduced synthesis of extracellular matrix proteins like type 1 collagen. [46,47] This can impair the vitality and activity of the bone matrix and subsequently lead to a reduction in the implant integration strength, which can contribute to aseptic prosthesis loosening. [48] Important components of the ECM expressed by osteoblasts are:

Collagen type I (COL1):

Osteoblasts create a layer of non-mineralized extracellular matrix, consisting of collagen fibrils and non-collagenous macromolecules, which are finally mineralized a few microns away from the cells. [49] Type I collagen is the predominant ECM component in bone, accounting for about 90% of the total proteins. [50,51] The mineralized collagen fibrils that serve as the basic building blocks of bone tissue are of indefinite length, insoluble, form sophisticated three-dimensional arrays and determine the mechanical properties of the bone. [49,52,53]

Osteopontin (SPP):

Osteopontin, a glycoprotein synthesized by both osteoblasts and osteoclasts, facilitates the adhesion of these cell types to the bone matrix, stimulates osteoclasts to migrate and resorb bone and plays an important role in matrix mineralization. [54-56]

Osteocalcin (BGLAP):

Osteocalcin, the most abundant non-collagenous protein in the bone matrix, is encoded by BGLAP and produced by the osteoblast. [57,58] Osteocalcin influences the mineralization and maturation of bones [59,60]. Ducy et al. have shown that the absence of osteocalcin in osteocalcin-deficient mice leads to increased bone formation without affecting bone resorption. [61] Furthermore, osteocalcin is believed to regulate glucose metabolism via a bone-pancreas endocrine loop [59] and is involved in the regulation of energy metabolism. [62,63]

1.6 Interleukins

Interleukins are a group of naturally occurring proteins that mediate communication between cells in order to regulate cell growth, differentiation, and motility. [64] They are particularly important in stimulating immune responses, such as inflammation. [64] Metal particles released from metallic prostheses can be phagocytosed by surrounding cells like osteoblasts and macrophages. [5,35,37] The implant debris-induced inflammation due to the innate immune system is caused predominantly by these cells, which react to aseptic implant debris releasing large quantities of proinflammatory cytokines and factors such as IL6, IL8, and tumor necrosis factor α (TNFα). [39,41,65,66] Most of these cytokines affect osteoclast differentiation and activity, and result in enhanced osteolysis. [32]

1.7 Matrix Metalloproteinases and their Inhibitors

Matrix metalloproteinases are enzymes with the capacity to degrade extracellular matrix components like collagen, aggrecan, elastin, and fibronectin. [67-70] They are synthesized as catalytically inactive pro-enzymes, and therefore require proteolytic activation occurring after the precise removal of an inhibitory pro-peptide. [68,69,71,72] MMPs can be classified according to their similarities in tridimensional structure and substrate affnity into six groups:

1) **collagenases** (MMPs -1, -8, and -13),
2) **gelatinases** (MMPs -2 and -9),
3) **stromelysins** (MMPs -3, -10 and -11),
4) **matrilysins** (MMPs -7 and -26),
5) **membrane-type metalloproteinases** (MMPs -14, -15, -16, -17, -24 and -25),
6) and **others** (MMPs - 12, -19, -20, -22, -23 and -28). [73]

Tissue inhibitors (TIMPs) are the physiologic inhibitors of MMPs in tissues and responsible for controlling the breakdown of ECM components by negatively modulating them, while the cell surface MMPs are inhibited by the RECK glycoprotein. [67,71,74,75] The balance between MMPs and their inhibitors is

essential for physiological ECM remodeling and imbalance of these enzymes leads to pathological states. [76] For identifying the function of MMPs, knockout mice for different MMPs have been generated and evaluated. [77-83] MMP-2 is preferentially found in osteoblasts and MMP-9 in osteoclasts. [74] MMP-2-null mice presented impaired bone matrix remodeling, a decrease in mineralization density of the tissue and an increase in porosity, suggesting that MMP-2 appears important to bone strength whereas MMP-9-null mice presented a decrease in structure, suggesting that MMP-9 appears important to bone toughness. [74,78,79,82] Holmbeck et al. reported that MT1-MMP (MMP-14) deficiency results in the loss of collagenolytic activity, scarring of joints and periskeletal tissues, reduced bone formation, and greatly enhanced bone resorptive activity, ultimately leading to a “vanishing bone” condition. [80] In pathological osteolysis observed in aseptic loosening of implants, the expression and synthesis of MMPs and TIMPs are thougt to be stimulated in osteoblasts directly by wear particle ingestion. [72]

1.8 Aim

According to our hypothesis, the above mentioned $TiAl_6V_4$ surface modifications can influence the geneexpression of osteoblasts and thus possibly contribute to aseptic prosthesis loosening. In the present diploma thesis, we therefore analysed the impact of this $TiAl_6V_4$ surface modifications on the expression of matrix metalloproteinases (MMP2, MMP9, MMP14) and their inhibitors (TIMP1, TIMP2) as well as the expression of Collagen typ I (COL1), Osteopontin (SPP) and Osteocalcin (BGLAP) in osteoblasts.

2 Methods and Materials

2.1 Scanning Electron Microscopy

For the Scanning electron microscopy (SEM) investigations a FEI Quanta 250 FEG (Thermo Fisher Scientific, Hillsboro, OR) was used. The scans were performed under vacuum conditions and 20 kV high voltage. The micrographs were recorded with an Everhart-Thornley-Detector. To ensure sufficient electrical conductivity, the surfaces were sputter-coated with a 10 nm gold layer. The measurements of energy dispersive X-ray spectroscopy (EDX) were performed for 60 s, under 20 kV high voltage. The EDX was measured with an Octane Elect Plus Silicon Drift Detector from EDAX Ametek, (NJ, USA) and APEX Standard Software V1.3.1. The following sample plates, which were used for our experiments, were examined:

$TiAl_6V_4$:

Wrought $TiAl_6V_4$ alloy consisting of titanium, 5.5 – 6.75% aluminum and 3.5–4.5% vanadium (supplied by implantcast GmbH, Buxtehude, Germany).

$TiAl_6V_4$+TiN:

The surface of the $TiAl_6V_4$ sample plates coated with titanium nitrid (supplied by implantcast GmbH) we used for our experiments is shown in figure 5. The sample plates were coated with a 5.5 ± 1.5 µm layer of titanium nitrid (TiN). The mean arithmetic average of the profile height (Ra) was <0.05 µm.

$TiAl_6V_4$+Ag:

The surface of the $TiAl_6V_4$ sample plates coated with silver (supplied by implantcast GmbH) we used for our experiments is shown in figure 6. The sample plates were coated with a 15 ± 5 µm layer of electrolytically deposited silver (Ag). The surface of the sample plates was sandblasted.

$TiAl_6V_4$ roughening:

The roughened surface of the $TiAl_6V_4$ sample plates (supplied by implantcast GmbH) we used for our experiments is shown in figure 7.

$TiAl_6V_4$+cpTi:

The surface of the $TiAl_6V_4$ sample plates coated with commercially pure Titanium (supplied by implantcast GmbH) we used for our experiments is shown in figure 8. The sample plates were coated with a 300 ± 50 µm layer of commercially pure Titanium (cpTi). The mean arithmetic average of the profile height (Ra) was 50 ± 15 µm and the porosity 30 ± 10%.

2.2 Cell Culture

For our in vitro investigation regarding the response of osteoblasts to surface modifications of $TiAl_6V_4$ metal alloys, we used hFOB1.19 osteoblasts (Homo sapiens, CRL-11372TM, ATCC, Manassas, VA) which we cultured in DMEM/F12 (GIBCO, Invitrogen, Darmstadt, Germany) cell culture media, supplemented with 10 % fetal bovine serum (FBS), 1 % L-glutamine, 100 units/mL penicillin and 100 µg/mL streptomycin (all GIBCO, Invitrogen, Darmstadt, Germany) at 34 °C in a humidified atmosphere with 5 % CO_2. The cell culture medium was changed every third day under aseptic conditions.

We performed seven experiments in total. Each of them was structured as follows:

1) We seeded the cells at a density of $5 * 10^4$ cells per well into a 24 well culture plate containing surface-modified discs consisting of $TiAl_6V_4$ and incubated it at 34°C for five days.

2) After the incubation period we performed a cytotoxicity assay, and

3) Isolated the RNA of the cells.

2.3 Seeding of hFOB cells on $TiAl_6V_4$ discs

The nutrient medium in the respective culture flask, which supplies the cells growing adherent at the bottom of the flask (see figure 2, A), was aspirated and the cells were separated from the bottom with trypsin. As soon as the cells were detached from the bottom of the bottle and floated around in the trypsin one by one (see figure 2, B), the trypsin was diluted with culture medium so that it did not damage the cells.

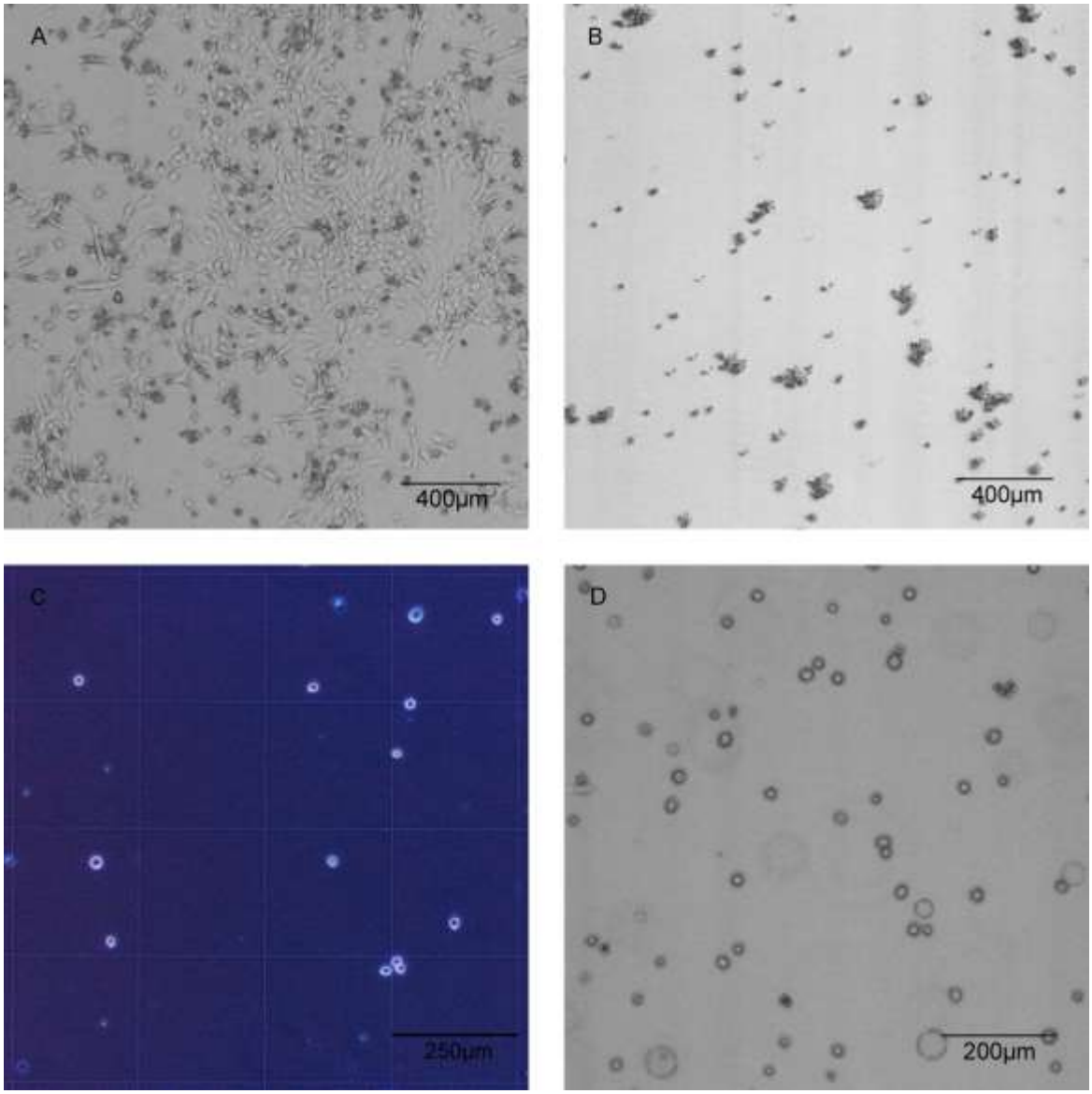

Figure 2:
Photomicrographs of hFOB: hFOB before removing the cells from the bottom of the culture flask (A). Spherical, freely floating cells detached from the bottom of the culture flask by trypsin (B). One of four fields of the hemocytometer for counting the cells after trypan blue staining (C). Cells placed in fresh culture medium for further cultivation (D).

The cell suspension was centrifuged, the supernatant was aspirated and the cell pellet was resuspended with a predetermined amount of culture media. A sample was taken, mixed with trypan blue in a 1:1 ratio and, using a hemocytometer, the approximate number of cells in the sample was determined (see figure 2, C). The cell suspension consisting of the cell pellet resuspended with nutrient medium, the approximate cell count of which was known now, was diluted with nutrient medium to obtain a suffcient amount of cell suspension to fill a 24 well culture plate completely with 1 ml per well containing 5 * 10^4 cells. For each experiment we used three pieces of these surface modificated sample plates of $TiAl_6V_4$ metal alloys respectively:

- $TiAl_6V_4$,
- $TiAl_6V_4$+TiN,
- $TiAl_6V_4$+Ag,
- $TiAl_6V_4$ roughening and
- $TiAl_6V_4$+cpTi.

Furthermore we used three sample plates of CoCrMo and three sample plates of PEEK in every experiment for comparison to $TiAl_6V_4$. All sample plates were delivered sterile sealed.

The sample plates were distributed to the wells according to the plan (see table 1) and the wells were filled. The filled 24 well culture plate was then incubated for five days at 34°C in a humified atmosphere with 5% CO_2.

CoCrMo Well 1	$TiAl_6V_4$ Well 1	$TiAl_6V_4$ + Ag Well 1	$TiAl_6V_4$ + TiN Well 1	$TiAl_6V_4$ + cpTi Well 1	$TiAl_6V_4$ rough Well 1
CoCrMo Well 2	$TiAl_6V_4$ Well 2	$TiAl_6V_4$ + Ag Well 2	$TiAl_6V_4$ + TiN Well 2	$TiAl_6V_4$ + cpTi Well 2	$TiAl_6V_4$ rough Well 2
CoCrMo Well 3	$TiAl_6V_4$ Well 3	$TiAl_6V_4$ + Ag Well 3	$TiAl_6V_4$ + TiN Well 3	$TiAl_6V_4$ + cpTi Well 3	$TiAl_6V_4$ rough Well 3
PEEK Well 1	PEEK Well 2	PEEK Well 3	Cells only Well 1	Cells only Well 2	Cells only Well 3

Table 1: Breadboard for seeding hFOB cells on $TiAl_6V_4$ discs.

The remaining cell suspension we filled into a culture flask with 20 ml fresh culture medium for further cultivation (see figure 2, D).

2.4 Cytotoxicity Assay

We measured the activity of Lactate Dehydrogenase (LDH) using the CytoTox-ONE Homogeneous Membrane Integrity Assay (Promega, Madison, MA).
After a five day incubation period, 100 µl of the cell culture supernatant were removed from each well of the 24 well culture plate of which 50 µl each were placed in two wells of a 96 well microtiter plate (see table 2). The cell culture supernatant of each well of the 96 well microtiter plate was mixed 1:1 with working solution and incubated in the dark for 10 minutes at room temperature.

	1	2	3	4	5	6	7	8	9	10	11	12
A	CoCrMo taken from well 1		$TiAl_6V_4$ taken from well 1		$TiAl_6V_4$ + Ag Taken from well 1		$TiAl_6V_4$ + TiN Taken from well 1		$TiAl_6V_4$ + cpTi Taken from well 1		$TiAl_6V_4$ rough Taken from well 1	
B	CoCrMo taken from well 2		$TiAl_6V_4$ taken from well 2		$TiAl_6V_4$ + Ag Taken from well 2		$TiAl_6V_4$ + TiN Taken from well 2		$TiAl_6V_4$ + cpTi Taken from well 2		$TiAl_6V_4$ rough Taken from well 2	
C	CoCrMo taken from well 3		$TiAl_6V_4$ taken from well 3		$TiAl_6V_4$ + Ag Taken from well 3		$TiAl_6V_4$ + TiN Taken from well 3		$TiAl_6V_4$ + cpTi Taken from well 3		$TiAl_6V_4$ rough Taken from well 3	
D	PEEK taken from well 1		Cells only taken from well 1									
E	PEEK taken from well 2		Cells only taken from well 1 and 2									
F	PEEK taken from well 3		Cells only taken from well 2									
G	Blank (nutrient medium)		Positiv control									
H												

Table 2: Breadboard for the Cytotoxicity assay.

50 µl of stop solution were admitted in order to stop the reaction and the fluorescence was measured at 560/590 nm using a Fluostar (BMC Labtech, Ortenberg, Germany).

2.5 RNA Isolation

The cell culture supernatant above the cells adhering to the bottom of each well of the 24 well culture plate was aspirated, 500 µl trypsin were put into each well to detach the cells from the bottom and the plate was incubated at 37 °C for about 5 minutes. Then 500 µl nutrient medium were filled into each well in order to dilute the trypsin. The fluids of each group of wells that was consisting of the three wells with idem plates were given into single 1,5 ml reaction tubes. After centrifugation of these tubes, the supernatant was aspirated and the cell pellet resuspended with 350 µl RLT-buffer and 350 µl ethanol to lyse the cells. For the suspension of each reaction tube that included the lyced cells of a group of three wells with idem plates one column from the RNeasy-Minikit (Qiagen, Hilden, Germany) was used.

For RNA purification we used the RNeasy-Minikit (Qiagen) following these worksteps:

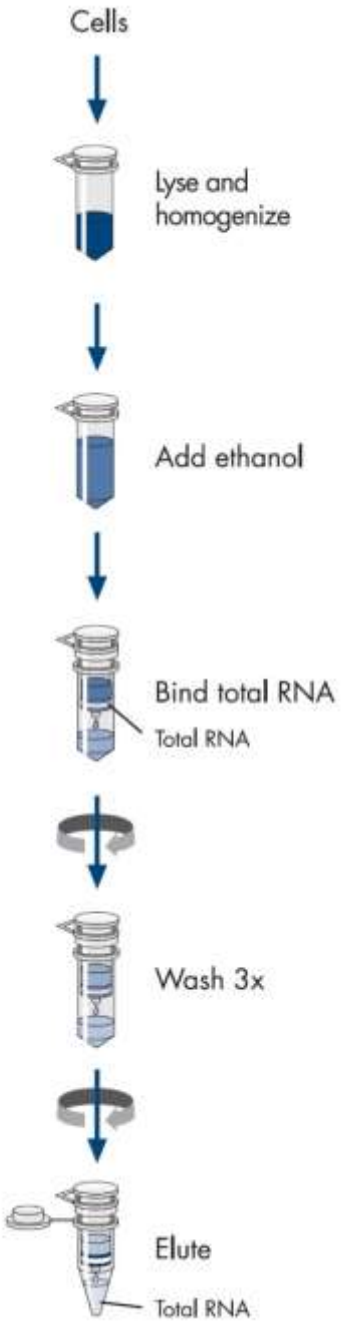

Figure 3:
RNeasy Mini procedure.
Adapted according to Qiagens
RNeasy mini Handbook
[84]

01) The suspensions were put onto the spin-columns.

02) The spin-columns were centrifuged at 10.000 rpm for 30 seconds and the liquid in the collection tubes was discarded.

03) 350µl of RW1 buffer were filled into each spin column.

04) The spin-columns were centrifuged at 10.000 rpm for 30 seconds and the liquid in the collection tubes was discarded.

05) Each spin-column was filled with 80µl incubation mix consisting of 70µl RDD buffer and 10µl DNase I stock solution and then incubated at room temperature for 15 minutes.

06) 350µl of RW1 buffer were filled into each spin column.

07) The spin-columns were centrifuged at 10.000 rpm for 30 seconds and the liquid in the collection tubes was discarded.

08) 500µl of RPE buffer were filled into each spin column.

09) The spin-columns were centrifuged at 10.000 rpm for 30 seconds and the liquid in the collection tubes was discarded.

10) 500µl of RPE buffer were filled into each spin column.

11) The spin-columns wers centrifuged at 10.000 rpm for 2 minutes and the liquid in the collection tubes was discarded.

12) The spin-columns were centrifuged at 13.000 rpm for 1 minute and put into new collection tubes.

13) 30µl of RNAse free water were filled into each spin column.

14) The spin-columns were centrifuged at 10.000 rpm for 1 minute to get the RNA into the collection tubes.

We quantified the samples using NanoDrop 2000 (Thermo Fisher Scientific, Waltham, MA, USA) and stored them in a frozen state.

2.6 c-DNA Synthesis

For further analysis of the gene expression we synthesized cDNA (complementary deoxyribonucleic acid) from the purified RNA samples using Biorad's iScript kit (Biorad, Hercules, California, USA). Per reaction we used 1µl reverse transcriptase (RT) to transcribe the single stranded RNA into cDNA, 4µl 5x iScript reaction mix (Biorad) and 1µg of the respective RNA template. This mix was filled up with NFW to a total volume of 20µl. We also prepared a No RT control (RT-) and a Negative control (NC) to enable the detection of contamination. The RT-control contained all components except the RT and was used for detection of contamination with residual genomic RNA. The NC contained all essential components for the reaction except the RNA template to detect contamination of the cDNA-synthesis kit. We incubated the reaction mix in a Thermocycler (myCycler, Biorad, Hercules, California, USA) as follows:

1) 5 min at 20°C . . . for annealing of the primers to the RNA.
2) 20 min at 46°C . . . for reverse transcription of RNA into cDNA.
3) 1 min at 94°C . . . for inactivation of the RT.

2.7 Real-Time PCR

For amplification and simultaneous measurement of the cDNA we used the method of Real-time PCR (RT-qPCR). We distributed the samples from each experiment on three 96 well plates. In each well we filled a mixture of 10µl consisting of

3 µl NFW,
1 µl of the respective primer,
1 µl of the respective cDNA template diluted to 12.5 ng/µl, and
5 µl of SsoAdvanced Universal SYBR Green Supermix (Biorad).

Each of the samples obtained from the cDNA synthesis was prepared as a triplicate, i.e. for each experiment, each cDNA - primer combination to be investigated was mixed three times as much as shown above and distributed over

three wells. In addition to the RT-qPCR of the cDNA templates, the following RT-qPCRs were performed for control purposes:

No RT control (RT-):

The mixture contains all components except the reverse transcriptase (RT). Instead of 1µl RT 1µl NFW is used. The no RT control is used for the detection of DNA contamination.

NC (negative control):

The mixture contains all components except the RNA template. Serves for the detection of contamination of the kit for c-DNA synthesis.

NTC (no tamplate control):

Contains all components for amplification except the cDNA template. The NTC is used for the detection of contaminations.

	B2M			RPL			MMP2			Control (RT-, NC, NTC)		
	1	2	3	4	5	6	7	8	9	10	11	12
A	B2M CoCrMo	B2M CoCrMo	B2M CoCrMo	RPL CoCrMo	RPL CoCrMo	RPL CoCrMo	MMP2 CoCrMo	MMP2 CoCrMo	MMP2 CoCrMo	RPL RT-	RPL RT-	RPL RT-
B	B2M $TiAl_6V_4$	B2M $TiAl_6V_4$	B2M $TiAl_6V_4$	RPL $TiAl_6V_4$	RPL $TiAl_6V_4$	RPL $TiAl_6V_4$	MMP2 $TiAl_6V_4$	MMP2 $TiAl_6V_4$	MMP2 $TiAl_6V_4$	RPL NC	RPL NC	RPL NC
C	B2M $TiAl_6V_4$ +TiN	B2M $TiAl_6V_4$ +TiN	B2M $TiAl_6V_4$ +TiN	RPL $TiAl_6V_4$ +TiN	RPL $TiAl_6V_4$ +TiN	RPL $TiAl_6V_4$ +TiN	MMP2 $TiAl_6V_4$ +TiN	MMP2 $TiAl_6V_4$ +TiN	MMP2 $TiAl_6V_4$ +TiN	B2M NTC	B2M NTC	B2M NTC
D	B2M $TiAl_6V_4$ +Ag	B2M $TiAl_6V_4$ +Ag	B2M $TiAl_6V_4$ +Ag	RPL $TiAl_6V_4$ +Ag	RPL $TiAl_6V_4$ +Ag	RPL $TiAl_6V_4$ +Ag	MMP2 $TiAl_6V_4$ +Ag	MMP2 $TiAl_6V_4$ +Ag	MMP2 $TiAl_6V_4$ +Ag	RPL NTC	RPL NTC	RPL NTC
E	B2M $TiAl_6V_4$ +cpTi	B2M $TiAl_6V_4$ +cpTi	B2M $TiAl_6V_4$ +cpTi	RPL $TiAl_6V_4$ +cpTi	RPL $TiAl_6V_4$ +cpTi	RPL $TiAl_6V_4$ +cpTi	MMP2 $TiAl_6V_4$ +cpTi	MMP2 $TiAl_6V_4$ +cpTi	MMP2 $TiAl_6V_4$ +cpTi	MMP2 NTC	MMP2 NTC	MMP2 NTC
F	B2M $TiAl_6V_4$ rough	B2M $TiAl_6V_4$ rough	B2M $TiAl_6V_4$ rough	RPL $TiAl_6V_4$ rough	RPL $TiAl_6V_4$ rough	RPL $TiAl_6V_4$ rough	MMP2 $TiAl_6V_4$ rough	MMP2 $TiAl_6V_4$ rough	MMP2 $TiAl_6V_4$ rough	MMP9 NTC	MMP9 NTC	MMP9 NTC
G	B2M $TiAl_6V_4$ PEEK	B2M $TiAl_6V_4$ PEEK	B2M $TiAl_6V_4$ PEEK	RPL $TiAl_6V_4$ PEEK	RPL $TiAl_6V_4$ PEEK	RPL $TiAl_6V_4$ PEEK	MMP2 $TiAl_6V_4$ PEEK	MMP2 $TiAl_6V_4$ PEEK	MMP2 $TiAl_6V_4$ PEEK	MMP14 NTC	MMP14 NTC	MMP14 NTC
H	B2M $TiAl_6V_4$ hFOB	B2M $TiAl_6V_4$ hFOB	B2M $TiAl_6V_4$ hFOB	RPL $TiAl_6V_4$ hFOB	RPL $TiAl_6V_4$ hFOB	RPL $TiAl_6V_4$ hFOB	MMP2 $TiAl_6V_4$ hFOB	MMP2 $TiAl_6V_4$ hFOB	MMP2 $TiAl_6V_4$ hFOB	TIMP1 NTC	TIMP1 NTC	TIMP1 NTC

Table 3: Representative depiction of the distribution of the samples on a 96 well plate.

After sticking the 96 well plates filled with the reaction mix with foil and centrifuging them for 1 minute at 900 x g, we incubated them in a thermocycler (CFX 96, Biorad, Hercules, California, USA) as follows:

1) 30 sec at 95°C . . . for polymerase activation and cDNA denaturation

2) 10 sec at 95°C . . . for denaturation

3) 20 sec at 60°C . . . for annealing/extension and plate read

40 cycles were performed.

For relative quantification we used the $\Delta\Delta C_T$-method:

1) From the fluorescence measurements, a Threshold cycle (C_T) is obtained for each sample, which is the cycle in which the first significant, detectable increase in fluorescence is observed.

2) The ΔC_T value is obtained by substracting from the C_T value of the target gene the C_T value of the respective reference gene.

3) The $\Delta\Delta C_T$ value is determined by substracting the ΔC_T value of the reference sample (which is $TiAl_6V_4$ in our case) from the ΔC_T value of the sample of interest.

4) The normalized target gene expression of each sample is $2^{-\Delta\Delta C_T}$.

3 Results

3.1 Surface Differences of the Sample Plates

The results of scanning electron microscopy (SEM) and its corresponding energy dispersive X-ray analysis (EDX) of the sample plates used for our experiments are shown in Figures 4-8. The microscopic SEM images illustrate the different surface morphology of the examined $TiAl_6V_4$ discs with differently modified surfaces. It is clearly visible that not only the roughened surface of $TiAl_6V_4$, but also the surfaces of $TiAl_6V_4$+TiN, and $TiAl_6V_4$+cpTi show considerably more unevenness than those of $TiAl_6V_4$ or $TiAl_6V_4$+Ag. The EDX analysis shows the clear differences between the types of surfaces in the composition of the chemical elements.

$TiAl_6V_4$:

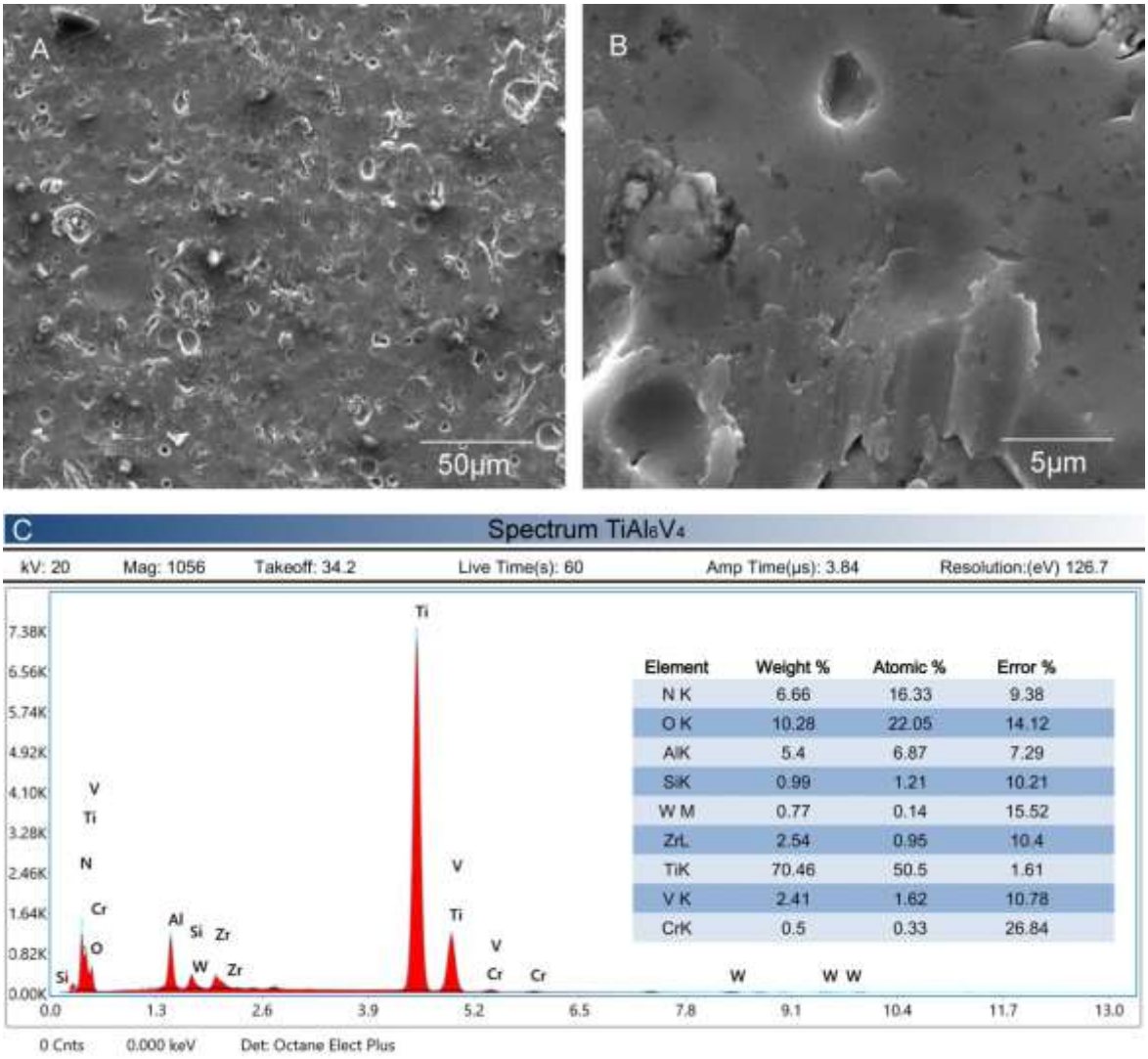

Figure 4:

Scanning electron microscopy (SEM) (A and B) and their corresponding energy-dispersive X-ray (EDX) (C) analysis of uncoated $TiAl_6V_4$ (1000x and 10.000x magnification). The pictures are used with the kind permission of Dr. Birgit Lohberger.

$TiAl_6V_4$+TiN:

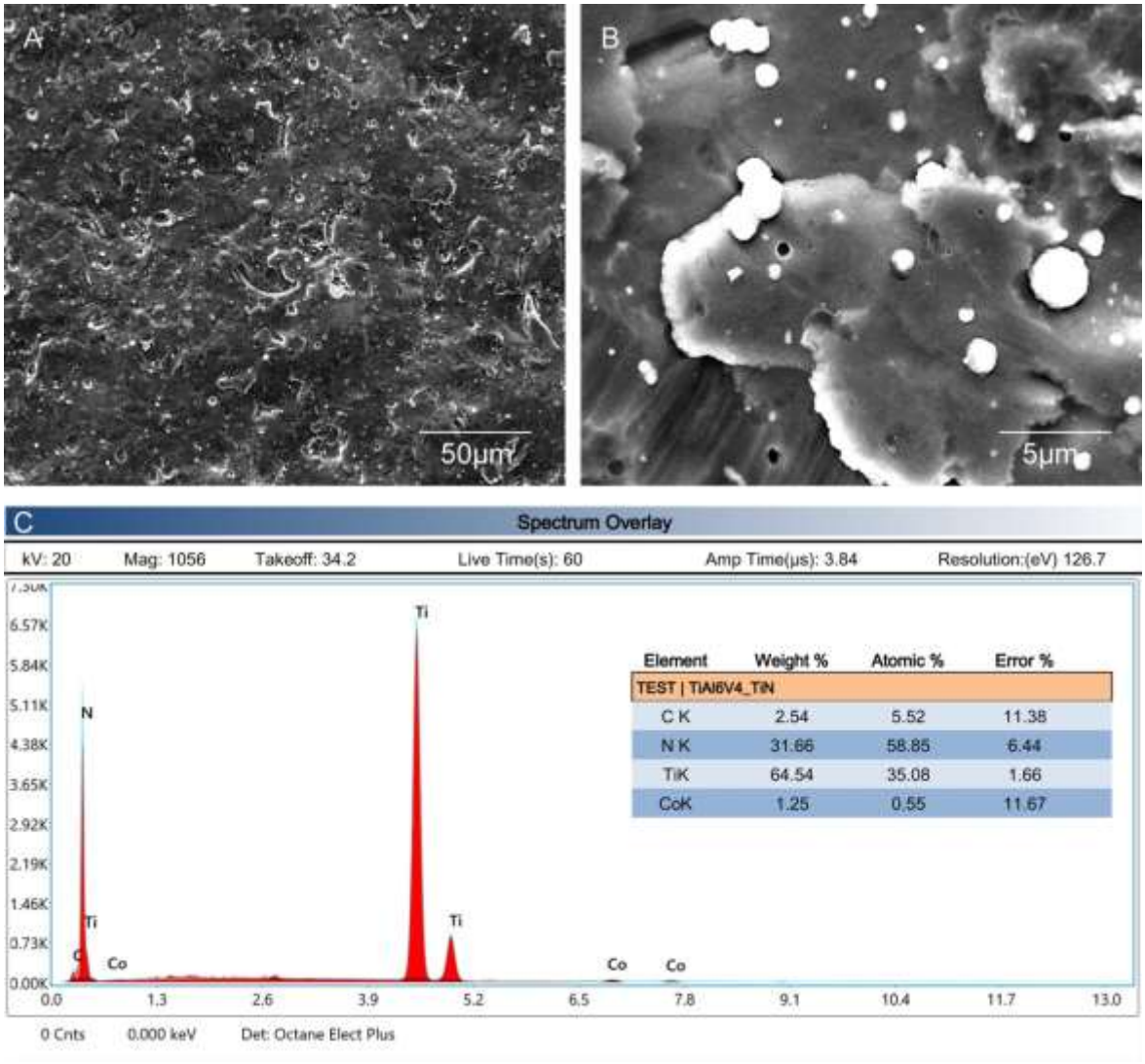

Figure 5:

Scanning electron microscopy (SEM) (A and B) and their corresponding energy-dispersive X-ray (EDX) (C) analysis of $TiAl_6V_4$ discs coated with TiN (1000x and 10.000x magnification). The pictures are used with the kind permission of Dr. Birgit Lohberger.

$TiAl_6V_4$+Ag:

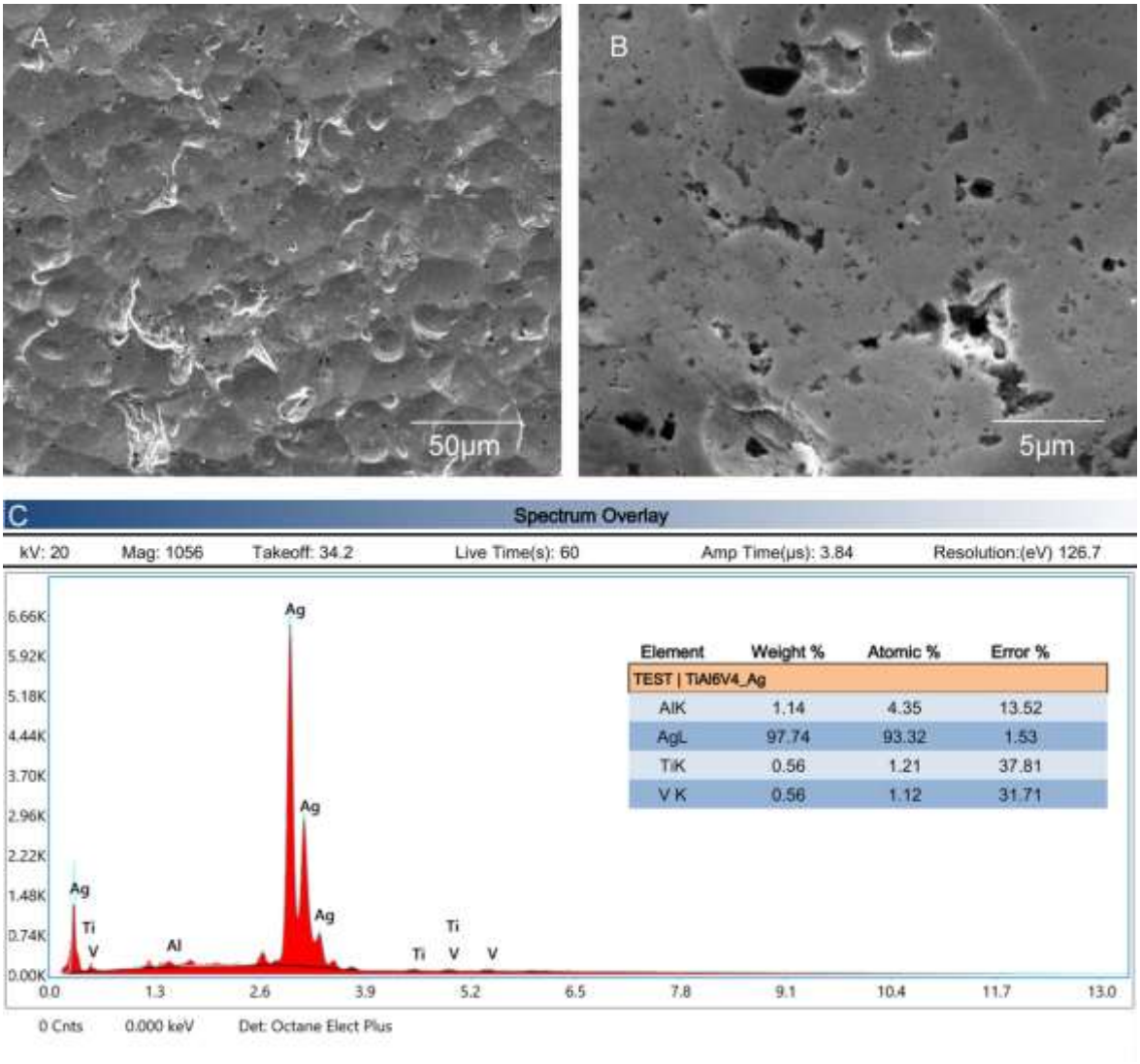

Figure 6:

Scanning electron microscopy (SEM) (A and B) and their corresponding energy-dispersive X-ray (EDX) (C) analysis of $TiAl_6V_4$ discs coated with Ag (1000x and 10.000x magnification). The pictures are used with the kind permission of Dr. Birgit Lohberger.

$TiAl_6V_4$ roughening:

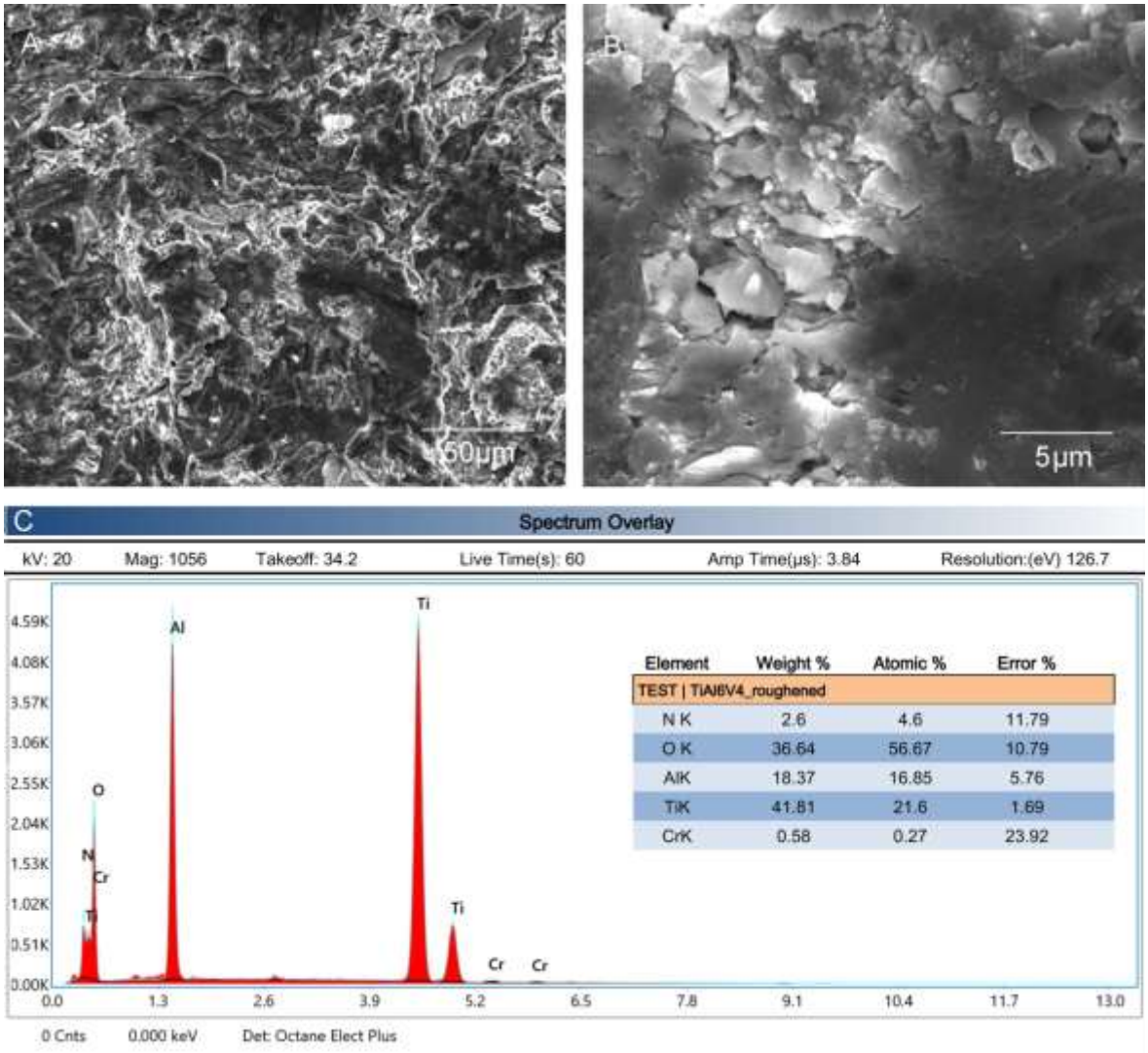

Figure 7:

Scanning electron microscopy (SEM) (A and B) and their corresponding energy-dispersive X-ray (EDX) (C) analysis of roughened $TiAl_6V_4$ discs (1000x and 10.000x magnification). The pictures are used with the kind permission of Dr. Birgit Lohberger.

$TiAl_6V_4$+cpTi:

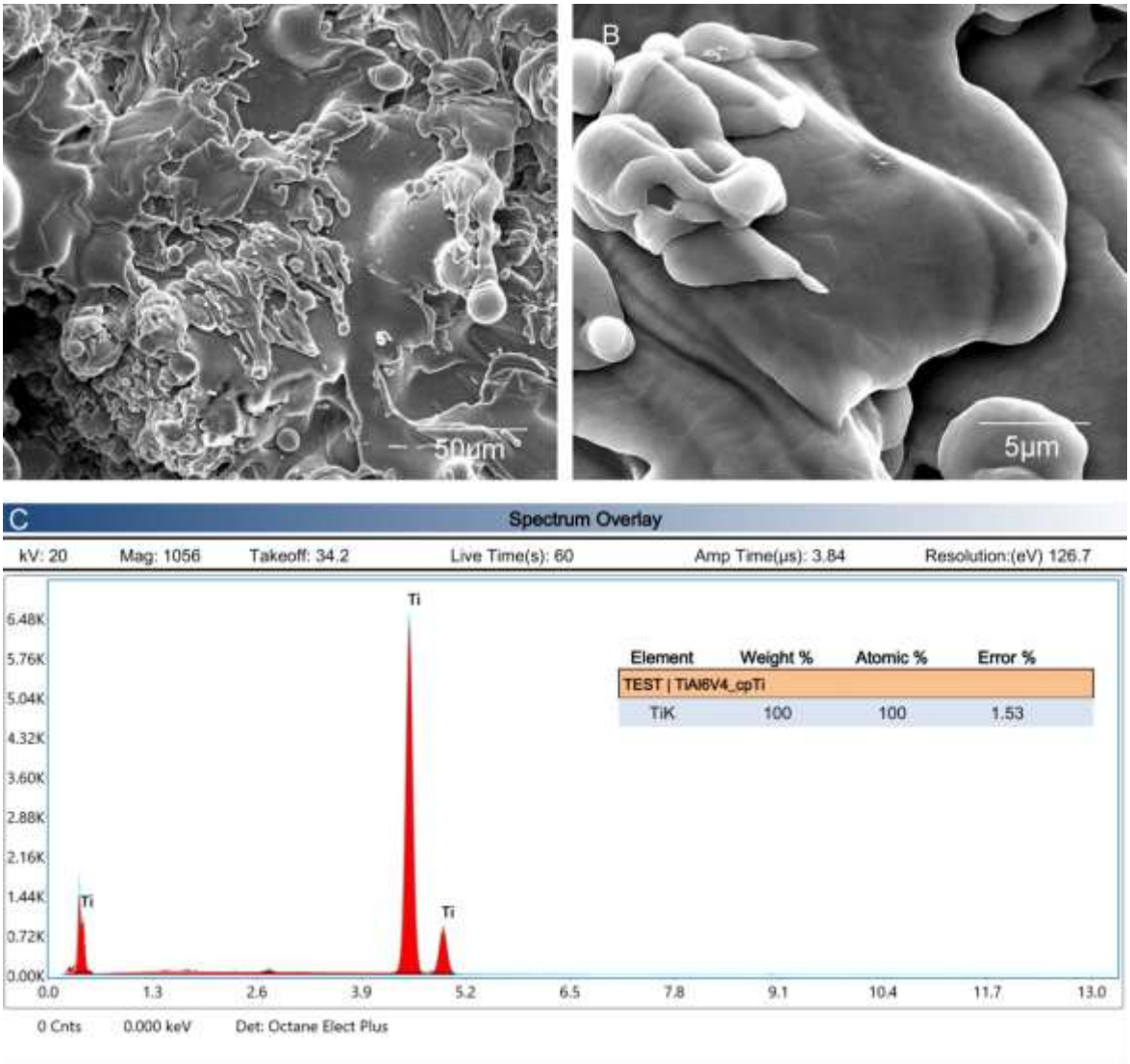

Figure 8:

Scanning electron microscopy (SEM) (A and B) and their corresponding energy-dispersive X-ray (EDX) (C) analysis of $TiAl_6V_4$ discs coated with cpTi (1000x and 10.000x magnification). The pictures are used with the kind permission of Dr. Birgit Lohberger.

3.2 Cytotoxicity Assay

We compared the fluorescence of the samples, which is proportional to the LDH loss of lysed cells, with the fluorescence of the positive control. We assumed a cytotoxicity of 100% for the positive control because we deliberately destroyed their cells, and compared the values (mean±SD; n=5) of the samples CoCrMo, $TiAl_6V_4$+TiN, $TiAl_6V_4$+Ag, $TiAl_6V_4$-roughening, $TiAl_6V_4$+cpTi, hFOB and PEEK with the values of $TiAl_6V_4$ using Student´s unpaired t-test. Except for the decline in the group of $TiAl_6V_4$+Ag the cytotoxicity assay showed no significant differences between the groups we examined. The cytotoxicity as a percentage of the positive control is shown in figure 9.

Cytotoxicity Assay:

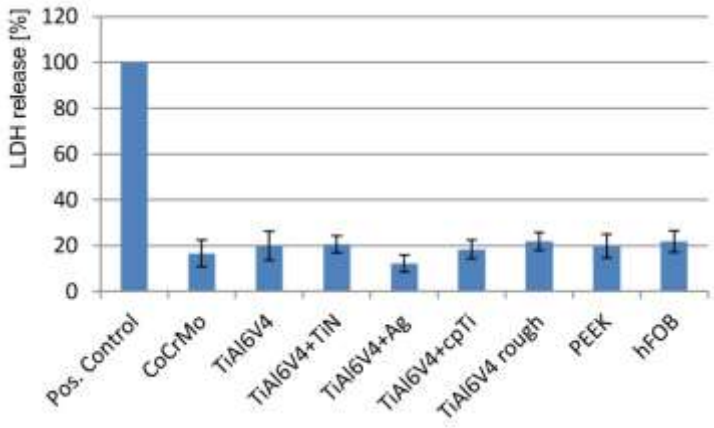

MMP2	mean	SD	p-value
Pos. Control	100	0.0	
CoCrMo	16.6	5.9	0.424
$TiAl_6V_4$	19.8	6.3	
$TiAl_6V_4$ + TiN	20.5	3.6	0.833
$TiAl_6V_4$ + Ag	12.2	3.6	**0.047**
$TiAl_6V_4$ + cpTi	18.3	4.0	0.670
$TiAl_6V_4$ rough	21.8	3.8	0.562
PEEK	19.8	5.2	0.998
hFOB	21.7	4.7	0.602

Figure 9:
Except for the decline in the group of $TiAl_6V_4$+Ag the cytotoxicity assay showed no significant differences between the groups we investigated and $TiAl_6V_4$ (p-values below 0.05 were considered significant; n=5).

3.3 Gene Expression

We compared the relative gene expression of MMP2, MMP9, MMP14, TIMP1, TIMP2, COL1, SPP and BGLAP both from cells (hFOB) grown on test plates of CoCrMo, $TiAl_6V_4$+TiN, $TiAl_6V_4$+Ag, $TiAl_6V_4$-roughening, $TiAl_6V_4$+cpTi and PEEK, as well as from cells growing without sample plates, with that of cells growing on plates of $TiAl_6V_4$. For evaluation we used Student´s one-sample t-test. P-values below 0.05 were considered significant. We compared the qPCR values from five experiments, which were measured as triplicates:

MMP2:

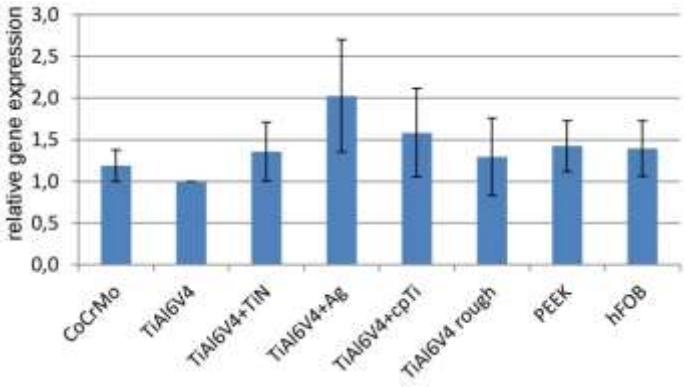

MMP2	mean	SD	p-value
CoCrMo	1.19	0.19	0.093
$TiAl_6V_4$ + TiN	1.36	0.35	0.087
$TiAl_6V_4$ + Ag	2.03	0.67	**0.027**
$TiAl_6V_4$ + cpTi	1.58	0.53	0.070
$TiAl_6V_4$ rough	1.29	0.46	0.229
PEEK	1.42	0.31	**0.036**
hFOB	1.39	0.33	0.058

Figure 10:
Compared to the $TiAl_6V_4$ control group the relative expression of MMP2 was significantly increased in the groups $TiAl_6V_4$+Ag and PEEK, whereas no significant difference was found in the groups CoCrMo, $TiAl_6V_4$+TiN, $TiAl_6V_4$+cpTi, $TiAl_6V_4$ rough and hFOB.

MMP9:

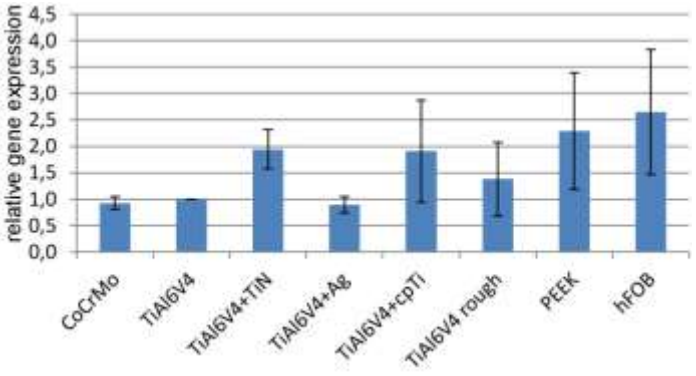

MMP9	mean	SD	p-value
CoCrMo	0.93	0.12	0.409
$TiAl_6V_4$ + TiN	1.94	0.37	**0.048**
$TiAl_6V_4$ + Ag	0.90	0.15	0.214
$TiAl_6V_4$ + cpTi	1.91	0.97	0.157
$TiAl_6V_4$ rough	1.38	0.69	0.291
PEEK	2.29	1.10	0.102
hFOB	2.65	1.18	0.068

Figure 11:

The expression of MMP9 in cells growing on CoCrMo, $TiAl_6V_4$+Ag, $TiAl_6V_4$+cpTi, $TiAl_6V_4$ rough, PEEK or hFOB was not different from that of cells growing on $TiAl_6V_4$ whereas the expression of MMP9 in cells growing on $TiAl_6V_4$+TiN was significantly higher than the expression of cells growing on $TiAl_6V_4$.

MMP14:

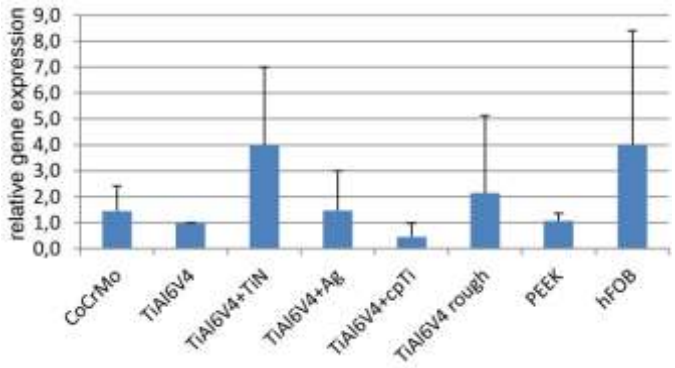

MMP14	mean	SD	p-value
CoCrMo	1.45	0.96	0.500
$TiAl_6V_4$ + TiN	3.98	3.02	0.229
$TiAl_6V_4$ + Ag	1.47	1.52	0.736
$TiAl_6V_4$ + cpTi	0.45	0.53	0.215
$TiAl_6V_4$ rough	2.15	2.98	0.574
PEEK	1.08	0.28	0.632
hFOB	4.02	4.38	0.355

Figure 12:

There were no significant differences in the expression of MMP14 in the groups investigated compared to the control group growing on $TiAl_6V_4$.

TIMP1:

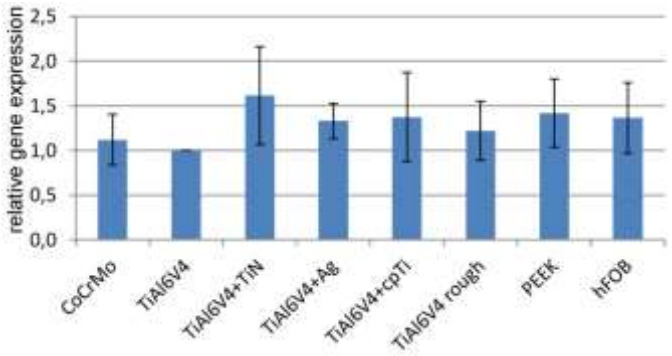

TIMP1	mean	SD	p-value
CoCrMo	1.12	0.28	0.463
$TiAl_6V_4$ + TiN	1.61	0.55	0.111
$TiAl_6V_4$ + Ag	1.33	0.20	**0.044**
$TiAl_6V_4$ + cpTi	1.37	0.50	0.231
$TiAl_6V_4$ rough	1.22	0.33	0.276
PEEK	1.42	0.38	0.118
hFOB	1.36	0.40	0.164

Figure 13:

A significantly higher expression of TIMP1 was found only in cells growing on $TiAl_6V_4$+Ag. All other cell groups investigated did not differ significantly from the control group in the expression of TIMP1.

TIMP2:

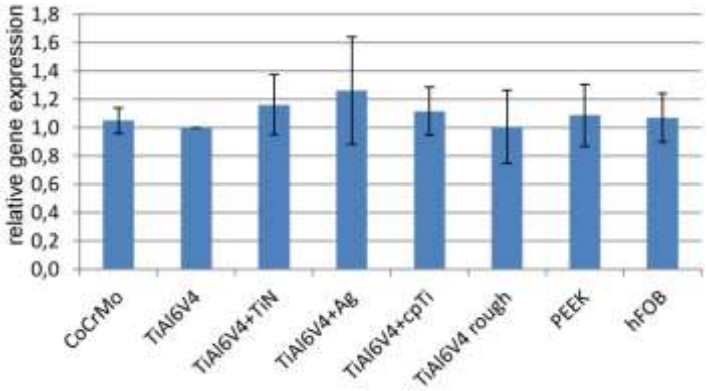

TIMP2	mean	SD	p-value
CoCrMo	1.05	0.09	0.285
$TiAl_6V_4$ + TiN	1.16	0.21	0.162
$TiAl_6V_4$ + Ag	1.26	0.38	0.198
$TiAl_6V_4$ + cpTi	1.12	0.17	0.198
$TiAl_6V_4$ rough	1.01	0.26	0.967
PEEK	1.09	0.22	0.422
hFOB	1.07	0.17	0.416

Figure 14:

There were no significant differences in the expression of TIMP2 between the investigated groups and the control group.

COL1:

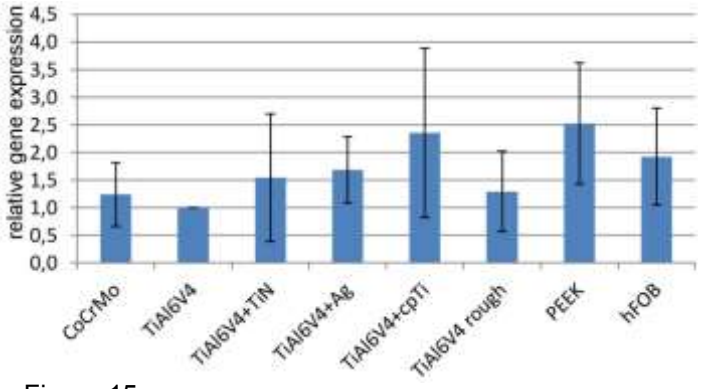

COL1	mean	SD	p-value
CoCrMo	1.24	0.57	0.406
$TiAl_6V_4$ + TiN	1.54	1.16	0.353
$TiAl_6V_4$ + Ag	1.68	0.60	0.107
$TiAl_6V_4$ + cpTi	2.35	1.53	0.174
$TiAl_6V_4$ rough	1.29	0.72	0.416
PEEK	2.52	1.10	0.069
hFOB	1.92	0.88	0.125

Figure 15:

Compared to the $TiAl_6V_4$ control group there were no significant differences in the relative expression of COL1.

SPP:

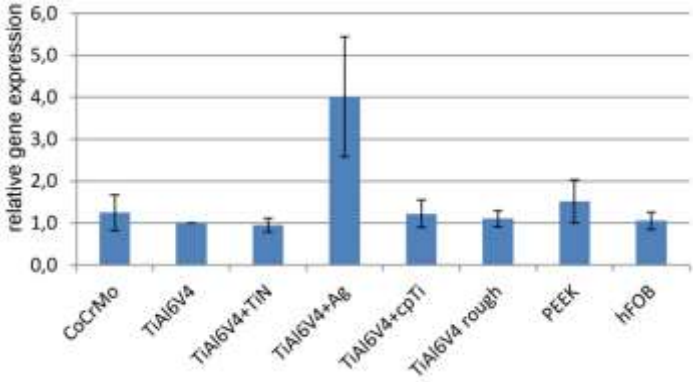

SPP	mean	SD	p-value
CoCrMo	1.25	0.43	0.264
$TiAl_6V_4$ + TiN	0.95	0.16	0.550
$TiAl_6V_4$ + Ag	4.01	1.44	**0.009**
$TiAl_6V_4$ + cpTi	1.22	0.33	0.209
$TiAl_6V_4$ rough	1.11	0.19	0.281
PEEK	1.51	0.51	0.088
hFOB	1.06	0.21	0.573

Figure 16:

Except for the increased SPP expression of those cells that grew on $TiAl_6V_4$+Ag, there were no significant differences in comparison to the control group growing on $TiAl_6V_4$.

BGLAP:

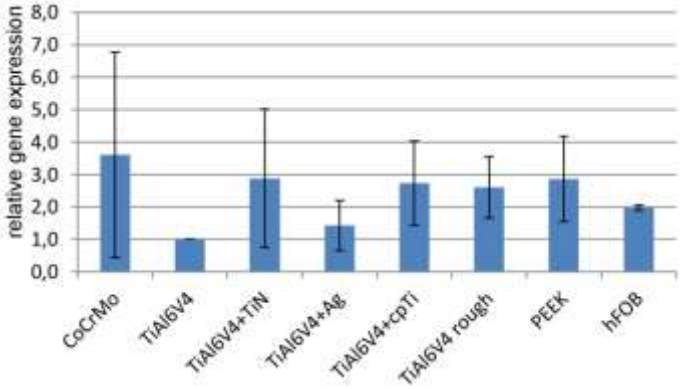

BGLAP	mean	SD	p-value
CoCrMo	3.61	3.16	0.288
$TiAl_6V_4$ + TiN	2.88	2.14	0.267
$TiAl_6V_4$ + Ag	1.43	0.77	0.441
$TiAl_6V_4$ + cpTi	2.74	1.29	0.146
$TiAl_6V_4$ rough	2.61	0.94	0.098
PEEK	2.86	1.31	0.134
hFOB	1.98	0.08	**0.002**

Figure 17:

Compared to the $TiAl_6V_4$ control group the relative expression of BGLAP was significantly increased in the group of hFOB, whereas no significant differences were found in the other groups.

4 Discussion

The reaction of bone-forming cells to implanted materials depends on their topography, chemical composition and surface roughness, as has been shown many times. [85-93] In the present diploma thesis we therefore analyzed the influence of $TiAl_6V_4$ surface modifications on both cytotoxicity and gene expression of matrix metalloproteinases (MMP2, MMP9, MMP14) and their inhibitors (TIMP1, TIMP2) as well as the expression of collagen type I (COL1), osteopontin (SPP) and osteocalcin (BGLAP) in osteoblasts (hFOB).

4.1 Cytotoxicity

The cytotoxicity of the investigated groups (CoCrMo, $TiAl_6V_4$, $TiAl_6V_4$+TiN, $TiAl_6V_4$+Ag, $TiAl_6V_4$-roughening, $TiAl_6V_4$+cpTi, hFOB and PEEK), with the exception of $TiAl_6V_4$+Ag, was about 20% of the level of cytotoxicity of the positive control. This value is comparable to the results of similar investigations that have been carried out with CoCrMo alloys. [94] Our examinations showed a significantly lower cytotoxicity for $TiAl_6V_4$+Ag compared to $TiAl_6V_4$. This is unexpected because surface coatings that contain larger amounts of Ag are known to have a cytotoxic effect in addition to their antibacterial effect. [95-101] The reason for the significantly lower measured values for cytotoxicity of $TiAl_6V_4$+Ag could be that the cells growing on $TiAl_6V_4$+Ag plates proliferated less. An indication for worse cell growth of hFOB on $TiAl_6V_4$+Ag is the concentration of isolated RNA of the $TiAl_6V_4$+Ag samples measured with nanodrop (not shown), which was considerably lower compared to the other samples. The cytotoxicity of all other investigated groups was similar to that of $TiAl_6V_4$. From this it can be concluded that neither the surface modification $TiAl_6V_4$+TiN, nor $TiAl_6V_4$+cpTi or $TiAl_6V_4$-roughening is associated with the risk of increased cytotoxicity.

4.2 Gene Expression

Based on the roughness of their surface, the sample plates can be broadly divided into two categories, whereby $TiAl_6V_4$-roughening, $TiAl_6V_4$+cpTi, and $TiAl_6V_4$+TiN are considered to belong to the category with an uneven surface and $TiAl_6V_4$ as well as $TiAl_6V_4$+Ag are considered to belong to the category with a more smooth surface. In the most comparable groups due to the same basic material ($TiAl_6V_4$ and $TiAl_6V_4$-roughening) no significant difference in the expression of the investigated genes could be found. From this it can be concluded that the chemical composition of the materials probably has a greater influence on the expression of MMP2, MMP9, MMP14, TIMP1, TIMP2, COL1, SPP and BGLAP than the structure of the surface.

hFOB cells growing on the sample plates CoCrMo, $TiAl_6V_4$+cpTi, or $TiAl_6V_4$-roughening did not show significant differences in the expression of MMP2, MMP9, MMP14, TIMP1, TIMP2, COL1, SPP or BGLAP compared to $TiAl_6V_4$.

MMPs are involved in establishing a balance between bone resorption and formation through their ability to cleave organic bone matrix. [68,70,102,103] Compared to the other samples, the very high C_T values of **MMP9** and **MMP14** (not shown) were prominent, indicating a very low expression of MMP9 and MMP14. This was observed, to a slightly varying degree, in all experiments performed on cells of all investigated groups. MMP14 was more or less equally represented in all groups without significant differences compared to $TiAl_6V_4$, while MMP9 was significantly more pronounced in the group $TiAl_6V_4$+TiN compared to $TiAl_6V_4$. Both the PEEK group and the $TiAl_6V_4$+Ag group showed significantly higher expression of **MMP2** than the $TiAl_6V_4$ group. Increased expression of MMPs, especially MMP2 which is known to cleave ECM components such as type 1 collagen [104,105], is generally thought to be linked to bone loss. [106-108] However, since the effects of MMPs are influenced at many levels, such as gene transcription, translation, secretion of inactive pro-enzymes, proteolytic activation, inhibition by specific inhibitors (such as TIMPs) or interaction with proteins of the extracellular matrix, MMP expression does not allow direct conclusions on their activity. [68] Although a comprehensive picture of the importance of MMPs for bone metabolism can be formed from various studies, the exact role of MMPs in periprosthetic osteolysis is still unclear. Therefore, the results of our investigations

about the influence of different surface modifications on the expression of MMPs can at the very most be interpreted as hints that can serve as a basis for further investigation in this field.

In the cell group growing on $TiAl_6V_4$+Ag, the expression of MMP2 as well as that of **TIMP1**, which is considered to be an inhibitor of MMP2 [109], and SPP was significantly increased compared to $TiAl_6V_4$. TIMPs are generelly known for their ability to inhibit the catalytic activity of MMPs in the ECM space. [76,110] A damage to the ECM caused by an increase of the expression of MMP2 would therefore rather be expected if the expression of TIMP1 were to decrease at the same time. In the expression of **TIMP2** no significant differences were observed between the groups we evaluated. This may be due to the constitutive expression pattern reported for TIMP2. [111]

The expression of **COL1**, which is necessary for the formation of mineralized bone matrix, was similar in all groups with no significant differences compared to $TiAl_6V_4$. The good expression of COL1 observed across all groups can be interpreted as an indication that none of the surface modifications studied, at least not by this pathway, negatively affects the formation of mineralized bone matrix.

A significantly higher expression of **BGLAP** was observed only in the hFOB group compared to the $TiAl_6V_4$ group. This can be seen as an indication that the production of osteocalcin is reduced in cells growing on $TiAl_6V_4$ surfaces.

The significantly higher expression of MMP2, TIMP1 and **SPP** in hFOB cells growing on $TiAl_6V_4$+Ag compared to $TiAl_6V_4$ could lead to the assumption that these cells produce increased amounts of ECM components such as SPP, which are cleaved by an increased release of MMPs (in this case MMP2) and the MMPs are controlled by an enhanced production of TIMPs. However, it should be noted that osteopontin (SPP) is not a known substrate of MMP2, in contrast to the most common protein of the ECM (COL1), which was not expressed at increased rates. Therefore, such a conclusion cannot be made on the basis of the present results and further investigation is necessary to determine whether or not there is a relationship.

In summary, the expression of MMP9 and MMP14 was generally very low, and with the exception of the group $TiAl_6V_4$+Ag compared to $TiAl_6V_4$ no significant differences in the expression of MMP2, TIMP1, TIMP2, COL1, SPP or BGLAP by hFOB cells growing on modificated surfaces of $TiAl_6V_4$ ($TiAl_6V_4$+TiN, $TiAl_6V_4$-roughening or $TiAl_6V_4$+cpTi) were found. From this it can be concluded that the above mentioned surface modifications have no significant influence on the expression of MMP2, TIMP1, TIMP2, COL1, SPP or BGLAP by osteoblasts and thus do not contribute to aseptic prosthesis loosening in this way. The effects of changes in the expression of MMP2, TIMP1 and SPP in hFOB cells growing on $TiAl_6V_4$+Ag and if there is a relationship between them is still to be investigated.

5 References

[1] Williams DF. On the nature of biomaterials. Biomaterials 2009; 30: 5897–5909.

[2] Park JB. Biomaterials Science and Engineering. New York: Plenum Press; 1984.

[3] Bertoluzza A. Raman Spectroscopy of Biomaterials Acting as Bone Prosthesis. In: Sandorfy C, Theophanides T, editors. Spectroscopy of Biological Molecules. Dordrecht: Springer; 1984. (NATO ASI Series C: Mathematical and Physical Sciences; vol 139).

[4] Park J, Lakes RS. Biomaterials: An introduction. 3rd ed. New York: Springer; 2007.

[5] Guglielmotti MB, Olmedo DG, Cabrini RL. Research on implants and osseointegration. Periodontol 2000. 2019; 79: 178–189.

[6] Gibon E, Amanatullah DF, Loi F, Pajarinen J, Nabeshima A, Yao Z et al. The biological response to orthopaedic implants for joint replacement: Part I: Metals. J Biomed Mater Res B Appl Biomater 2017; 105(7): 2162–2173.

[7] Koh J, Berger A, Benhaim P. An overview of internal fixation implant metallurgy and galvanic corrosion effects. J Hand Surg Am 2015; 40: 1703–1710.

[8] Navarro M, Michiardi A, Castano O, Planell JA. Biomaterials in orthopaedics. J R Soc Interface 2008; 5: 1137–1158.

[9] Niinomi M, Boehlert CJ. Titanium Alloys for Biomedical Applications. In: Niinomi M, Narushima T, Nakai M, editors. Advances in metallic biomaterials: Tissues, materials and biological reactions. Berlin Heidelberg: Springer; 2015. p.179–215. (Springer Series in Biomaterials Science and Engineering; vol 3)

[10] Long M, Rack HJ. Titanium alloys in total joint replacement – a materials science perspective. Biomaterials 1998; 19: 1621–1639.

[11] Kaur M, Singh K. Review on titanium and titanium based alloys as biomaterials for orthopaedic applications. Mater Sci Eng C 2019; 102: 844–862.

[12] Geetha M, Singh AK, Asokamani R, Gogia AK. Ti based biomaterials, the ultimate choice for orthopaedic implants – a review. Prog Mater Sci 2009; 54: 397–425.

[13] Liu Y, Rath B, Tingart M, Eschweiler J. Role of implants surface modification in osseointegration: A systematic review. J Biomed Mater Res 2020; 108A: 470–484.

[14] Takemoto M, Fujibayashi S, Neo M, Suzuki J, Kokubo T, Nakamura T. Mechanical properties and osteoconductivity of porous bioactive titanium. Biomaterials 2005; 26: 6014–6023.

[15] Kim Y. Intermetallic alloys based on gamma titanium aluminide. JOM 1989; 41: 24–30.

[16] Leyens C, Peters M, editors. Titanium and titanium alloys: fundamentals and applications. Weinheim: Wiley-vch; 2003.

[17] Ponader S, Vairaktaris E, Heinl P, Wilmowsky C, Rottmair A, Körner C et al. Effects of topographical surface modifications of electron beam melted Ti-6Al-4V titanium on human fetal osteoblasts. J Biomed Mater Res 2007; A84: 1111–1119.

[18] Bagno A, Di Bello C. Surface treatments and roughness properties of Ti-based biomaterials. J Mater Sci Mater Med 2004; 15: 935–949.

[19] Ozdemir Z, Ozdemir A, Basim GB. Application of chemical mechanical polishing process on titanium based implants. Mater Sci Eng 2019; C68: 383–396.

[20] Hinüber C, Kleemann C, Friederichs RJ, Haubold L, Scheibe HJ, Schuelke T et al. Biocompatibility and mechanical properties of diamond-like coatings on cobalt-chromium-molybdenum steel and titanium-aluminum-vanadium biomedical alloys. J Biomed Mater Res Part A 2010; 95(2): 388–400.

[21] van Hove RP, Sierevelt IN, van Royen BJ, Nolte PA. Titanium-Nitride Coating of Orthopaedic Implants: A Review of the Literature. BioMed Res Int 2015; vol 2015: 485975.

[22] Fabry C, Zietz C, Baumann A, Ehall R, Bader R. High wear resistance of femoral components coated with titanium nitride: a retrieval analysis. Knee Surg Sports Traumatol Arthrosc 2017: 1–10.

[23] De Giglio E, Cafagna D, Cometa S, Allegretta A, Pedico A, Giannossa LC et al. An innovative, easily fabricated, silver nanoparticle-based titanium implant coating: Development and analytical characterization. Anal Bioanal Chem 2013; 405: 805–816.

[24] Kargupta R, Bok S, Darr CM, Crist BD, Gangopadhyay K, Gangopadhyay S et al. Coatings and surface modifications imparting antimicrobial activity to orthopedic implants. WIREs Nanomed Nanobiotechnol 2014; 6: 475–495.

[25] Goyal E, Kapoor D, Soni N, Jain R. Osseointegration- A Review. Arch of Dent and Med Res 2016; 2(1): 9–14.

[26] Kubies D, Himmlova L, Riedel T, Chanova E, Balik K, Douderova M et al. The interaction of osteoblasts with bone-implant materials: 1. The effect of physicochemical surface properties of implant materials. Physiol Res 2011; 60: 95–111.

[27] Shah FA, Trobos M, Thomsen P, Palmquist A. Commercially pure titanium (cp-Ti) versus titanium alloy (Ti6Al4V) materials as bone anchored implants - Is one truly better than the other? Mater Sci Eng C Mater Biol Appl 2016; 62: 960–966.

[28] Mavrogenis AF, Dimitriou R, Parvizi J, Babis GC. Biology of implant osseointegration. J Musculoskelet Neuronal Interact 2009; 9(2): 61-71.

[29] Schwartz AM, Farley KX, Guild GN, Bradbury TL. Projections and Epidemiology of Revision Hip and Knee Arthroplasty in the United States to 2030. The Journal of Arthroplasty 2020: 1–7.

[30] Halvorsen V, Fenstad AM, Engsaeter LB, Nordsletten L, Overgaard S, Pedersen AB et al. Outcome of 881 total hip arthroplasties in 747 patients 21 years or younger: data from the Nordic Arthroplasty Register Association (NARA) 1995–2016. Acta Orthopaedica 2019; 90(4): 331–337.

[31] Holt G, Murnaghan C, Reilly J, Meek RM. The biology of aseptic osteolysis. Clin Orthop Relat Res 2007; 460: 240-252.

[32] Abu-Amer Y, Darwech I, Clohisy J. Aseptic loosening of total joint replacements: mechanisms underlying osteolysis and potential therapies. Arthritis Research & Therapy. 2007; 9: 1–7.

[33] Gwam CU, Mistry JB, Mohamed NS, Thomas M, Bigart K, Mont MA et al. Current Epidemiology of Revision Total Hip Arthroplasty in the United States: National Inpatient Sample 2009 to 2013. The Journal of Arthroplasty 2017; 32: 2088–2092.

[34] Purdue PE, Koulouvaris P, Potter HG, Nestor BJ, Sculco TP. The Cellular and Molecular Biology of Periprosthetic Osteolysis. Clin Orthop Relat Res 2006; 454: 251–261.

[35] Hallab NJ, Jacobs JJ. Biologic effects of implant debris. Bull NYU Hosp Jt Dis 2009; 67: 182–188.

[36] Tiddens OWT. Definition der histologischen Kriterien zur Differenzierung zwischen aseptischer und septischer Prothesenlockerung. Charité - Universitätsmedizin Berlin; 2013. Available at: https://refubium.fu-berlin.de/handle/fub188/266
Accessed September 25, 2020.

[37] Lohmann CH, Schwartz Z, Köster G, Jahn U, Buchhorn GH, MacDougall MJ et al. Phagocytosis of wear debris by osteoblasts affects differentiation and local factor production in a manner dependent on particle composition. Biomaterials 2000; 21: 551–561.

[38] Jacobs JJ, Gilbert JL, Urban RM. Corrosion of metal orthopaedic implants. J Bone Joint Surg Am 1998; 80: 268–282.

[39] O'Neill SC, Queally JM, Devitt BM, Doran PP, O'Byrne JM. The role of osteoblasts in peri-prosthetic Osteolysis. Bone Joint J 2013; 95-B: 1022-1026.

[40] Costa BC, Tokuhara CK, Rocha LA, Oliveira RC, Lisboa-Filho PN, Pessoa JC. Vanadium ionic species from degradation of Ti-6Al-4V metallic implants: In vitro cytotoxicity and speciation evaluation. Mater Sci Eng C 2019; 96: 730–739.

[41] Caicedo MS, Pennekamp PH, McAllister K, Jacobs JJ, Hallab NJ. Soluble ions more than particulate cobaltalloy implant debris induce monocyte costimulatory molecule expression and release of proinflammatory cytokines critical to metal-induced lymphocyte reactivity. J Biomed Mater Res A 2010; 93(4): 1312–1321.

[42] Hallab NJ, Cunningham BW, Jacobs JJ. Spinal implant debris-induced osteolysis. Spine 2003; 28: 125–138.

[43] Currey JD. The design of mineralised hard tissues for their mechanical functions. J Exp Biol. 1999; 202(Pt 23): 3285–3294.

[44] Gentili C, Cancedda R. Cartilage and bone extracellular matrix. Curr Pharm Des. 2009; 15(12): 1334–1348.

[45] Alliston T. Biological regulation of bone quality. Curr Osteoporos Rep. 2014; 12(3): 366–375.

[46] Lochner K, Fritsche A, Jonitz A, et al. The potential role of human osteoblasts for periprosthetic osteolysis following exposure to wear particles. Int J Mol Med. 2011; 28(6): 1055–1063.

[47] Wang ML, Nesti LJ, Tuli R, et al. Titanium particles suppress expression of osteoblastic phenotype in human mesenchymal stem cells. J Orthop Res. 2002; 20(6): 1175–1184.

[48] Syggelos SA, Aletras AJ, Smirlaki I, Skandalis SS. Extracellular matrix degradation and tissue remodeling in periprosthetic loosening and osteolysis: focus on matrix metalloproteinases, their endogenous tissue inhibitors, and the proteasome. Biomed Res Int. 2013; 2013: 230805.

[49] Beniash E. Biominerals--hierarchical nanocomposites: the example of bone. Wiley Interdiscip Rev Nanomed Nanobiotechnol. 2011; 3(1): 47–69.

[50] Gorski JP. Biomineralization of bone: a fresh view of the roles of non-collagenous proteins. Front Biosci (Landmark Ed). 2011; 16: 2598–2621.

[51] Ida T, Kaku M, Kitami M, et al. Extracellular matrix with defective collagencross-linking affects the differentiation of bone cells. PLoS One. 2018; 13(9): e0204306. Published 2018 Sep 25.

[52] Canty EG, Kadler KE. Procollagen trafficking, processing and fibrillogenesis. J Cell Sci. 2005; 118(Pt 7): 1341–1353.

[53] Georgiadis M, Müller R, Schneider P. Techniques to assess bone ultrastructure organization: orientation and arrangement of mineralized collagen fibrils. J R Soc Interface. 2016; 13(119): 20160088.

[54] Giachelli CM, Steitz S. Osteopontin: a versatile regulator of inflammation and biomineralization. Matrix Biol. 2000; 19(7): 615–622.

[55] Sodek J, Gnass B, McKee MD. Osteopontin. Crit Rev Oral Biol Med. 2000; 11(3): 279–303.

[56] Zhou S, Zu Y, Sun Z, Zhuang F, Yang C. Effects of Hypergravity on Osteopontin Expression in Osteoblasts. PLoS One. 2015; 10(6): e0128846.

[57] Hauschka PV, Lian JB, Cole DE, Gundberg CM. Osteocalcin and matrix Gla protein: vitamin K-dependent proteins in bone. Physiol Rev. 1989; 69(3): 990–1047.

[58] Dirckx N, Moorer MC, Clemens TL, Riddle RC. The role of osteoblasts in energy homeostasis. Nat Rev Endocrinol. 2019; 15(11): 651–665.

[59] Zoch ML, Clemens TL, Riddle RC. New insights into the biology of osteocalcin. Bone. 2016; 82: 42–49.

[60] Boskey AL, Gadaleta S, Gundberg C, Doty SB, Ducy P, Karsenty G. Fourier transform infrared microspectroscopic analysis of bones of osteocalcin-deficient mice provides insight into the function of osteocalcin. Bone. 1998; 23(3): 187–196.

[61] Ducy P, Desbois C, Boyce B, et al. Increased bone formation in osteocalcin-deficient mice. Nature. 1996; 382(6590): 448–452.

[62] Lee NK, Sowa H, Hinoi E, et al. Endocrine regulation of energy metabolism by the skeleton. Cell. 2007; 130(3): 456–469.

[63] Wei J, Karsenty G. An overview of the metabolic functions of osteocalcin. Rev Endocr Metab Disord. 2015; 16(2): 93–98.

[64] Interleukin. In: Encyclopaedia Britannica. Encyclopaedia Britannica, Inc.; 21 August 2019. Available at: https://www.britannica.com/science/interleukin. Accessed April 18, 2020.

[65] Hallab NJ, Jacobs JJ. Chemokines Associated with Pathologic Responses to Orthopedic Implant Debris. Front Endocrinol 2017; 8;5.

[66] Christiansen RJ, Münch HJ, Bonefeld CM, Thyssen JP, Sloth JJ, Geisler C et al. Cytokine profile in patients with aseptic loosening of total hip replacements and its relation to metal release and metal allergy. J Clin Med 2019, 8, 1259.

[67] Nagase H, Woessner JF. Matrix Metalloproteinases. J Biol Chem 1999; 274: 21491–21494.

[68] Hardy E, Fernandez-Patron C. Destroy to Rebuild: The Connection Between Bone Tissue Remodeling and Matrix Metalloproteinases. Front Physiol 2020; 11:47.

[69] Filanti C, Dickson GR, Di Martino D, Ulivi V, Sanguineti C, Romano P et al. The expression of metalloproteinase-2, -9, and -14 and of tissue inhibitors-1 and -2 is developmentally modulated during osteogenesis in vitro, the mature osteoblastic phenotype expressing metalloproteinase-14. J Bone Miner Res 2000; 15(11): 2154–2168.

[70] Laronha H, Caldeira J. Structure and Function of Human Matrix Metalloproteinases. Cells 2020; 9, 1076.

[71] Tokuhara CK, Santesso MR, Oliveira GSN, Ventura TMDS, Doyama JT, Zambuzzi WF et al. Updating the role of matrix metalloproteinases in mineralized tissue and related diseases. J Appl Oral Sci 2019; 27, e20180596.

[72] Oumhamed Z, Garnotel R, Josset Y, Trenteseaux C, Laurent-Maquin D. Matrix metalloproteinases MMP-2, -9 and tissue inhibitors TIMP-1, -2 expression and secretion by primary human osteoblast cells in response to t itanium, zirconia, and alumina ceramics. J Biomed Mater Res A 2004; 68: 114–122.

[73] Visse R, Nagase H. Matrix metalloproteinases and tissue inhibitors of metalloproteinases: structure, function, and biochemistry. Circ Res 2003; 92(8): 827–839.

[74] Paiva KBS, Granjeiro JM, Bone tissue remodeling and development: Focus on matrix metalloproteinase functions. Archives of Biochemistry and Biophysics 2014; 561: 74–87.

[75] Takahashi C, Sheng Z, Horan TP, Kitayama H, Maki M, Hitomi K et al. Regulation of matrix metalloproteinase-9 and inhibition of tumor invasion by the membrane-anchored glycoprotein RECK. Proc Natl Acad Sci U S A. 1998; 95: 13221–13226.

[76] Paiva KBS, Granjeiro JM. Matrix metalloproteinases in bone resorption, remodelling, and repair. Prog Mol Biol Transl Sci 2017; 148: 203–303.

[77] Inada M, Wang Y, Byrne MH, Rahman MU, Miyaura C, Lo pez-Otin C et al. Critical roles for collagenase-3 (Mmp13) in development of growth plate cartilage and in endochondral ossification. Proc Natl Acad Sci USA 2004; 101: 17192–17197.

[78] Inoue K, Mikuni-Takagaki Y, Oikawa K, Itoh T, Inada M, Noguchi T et al. A crucial role for matrix metalloproteinase 2 in osteocytic canalicular formation and bone metabolism. J Biol Chem 2006; 281: 33814–33824.

[79] Mosig RA, Dowling O, DiFeo A, Ramirez MCM, Parker IC, Abe E et al. Loss of MMP-2 disrupts skeletal and craniofacial development, and results in decreased bone mineralization, joint erosion, and defects in osteoblast and osteoclast growth. Hum Mol Genet 2007; 16(9): 1113–1123.

[80] Holmbeck K, Bianco P, Yamada S, Birkedal-Hansen H. MT1-MMP: a tethered collagenase. J Cell Physiol 2004; 200: 11–19.

[81] Holmbeck K, Bianco P, Pidoux I, Inoue S, Billinghurst RC, Wu W et al. The metalloproteinase MT1-MMP is required for normal development and maintenance of osteocyte processes in bone. J Cell Sci 2005; 118: 147–156.

[82] Vu TH, Shipley JM, Bergers G, Berger JE, Helms JA, Hanahan D et al. MMP-9/gelatinase B is a key regulator of growth plate angiogenesis and apoptosis of hypertrophic chondrocytes. Cell 1998; 93: 411–422.

[83] Stickens D, Behonick DJ, Ortega N, Heyer B, Hartenstein B, Yu Y et al. Altered endochondral bone development in matrix metalloproteinase 13-deficient mice. Development. 2004; 131: 5883–5895.

[84] Quiagen. RNeasy Mini Handbook 10/2019. Available at: https://www.qiagen.com/us/resources/resourcedetail?id=14e7cf6e-521a-4cf7-8cbc-bf9f6fa33e24&lang=en
Accessed Mai 16, 2020.

[85] Lukaszewska-Kuska M, Wirstlein P, Majchrowski R, Dorocka-Bobkowska B. Osteoblastic cell behaviour on modified titanium surfaces. Micron. 2018; 105: 55–63.

[86] Bächle M, Kohal RJ. A systematic review of the influence of different titanium surfaces on proliferation, differentiation and protein synthesis of osteoblast-like MG63 cells. Clin Oral Implants Res. 2004; 15(6): 683–692.

[87] Liu R, Ma Z, Kunle Kolawole S, et al. In vitro study on cytocompatibility and osteogenesis ability of Ti-Cu alloy. J Mater Sci Mater Med. 2019; 30(7): 75.

[88] Lincks J, Boyan BD, Blanchard CR, et al. Response of MG63 osteoblast-like cells to titanium and titanium alloy is dependent on surface roughness and composition. Biomaterials. 1998; 19(23): 2219–2232.

[89] Perrotti V, Palmieri A, Pellati A, et al. Effect of titanium surface topographies on human bone marrow stem cells differentiation in vitro. Odontology. 2013; 101(2): 133–139.

[90] Yin C, Zhang Y, Cai Q, et al. Effects of the micro-nano surface topography of titanium alloy on the biological responses of osteoblast. J Biomed Mater Res A. 2017; 105(3): 757–769.

[91] Sista S, Wen C, Hodgson PD, Pande G. Expression of cell adhesion and differentiation related genes in MC3T3 osteoblasts plated on titanium alloys: role of surface properties. Mater Sci Eng C Mater Biol Appl. 2013; 33(3): 1573–1582.

[92] Setzer B, Bächle M, Metzger MC, Kohal RJ. The gene-expression and phenotypic response of hFOB 1.19 osteoblasts to surface-modified titanium and zirconia. Biomaterials. 2009; 30(6): 979–990.

[93] Park JW, Kim HK, Kim YJ, Jang JH, Song H, Hanawa T. Osteoblast response and osseointegration of a Ti-6Al-4V alloy implant incorporating strontium. Acta Biomater. 2010; 6(7): 2843–2851.

[94] Lohberger B, Stuendl N, Glaenzer D, et al. CoCrMo surface modifications affect biocompatibility, adhesion, and inflammation in human osteoblasts. Sci Rep. 2020; 10(1): 1682.

[95] Lubick N. Nanosilver toxicity: ions, nanoparticles - or both?. Environ Sci Technol. 2008; 42(23): 8617.

[96] Kim S, Ryu DY. Silver nanoparticle-induced oxidative stress, genotoxicity and apoptosis in cultured cells and animal tissues. J Appl Toxicol. 2013; 33(2): 78–89.

[97] Mijnendonckx K, Leys N, Mahillon J, Silver S, Van Houdt R. Antimicrobial silver: uses, toxicity and potential for resistance. Biometals. 2013; 26(4): 609–621.

[98] Croes M, Bakhshandeh S, van Hengel IAJ, et al. Antibacterial and immunogenic behavior of silver coatings on additively manufactured porous titanium. Acta Biomater. 2018; 81: 315–327.

[99] Necula BS, van Leeuwen JP, Fratila-Apachitei LE, Zaat SA, Apachitei I, Duszczyk J. In vitro cytotoxicity evaluation of porous TiO_2-Ag antibacterial coatings for human fetal osteoblasts. Acta Biomater. 2012; 8(11): 4191–4197.

[100] Yamamoto A, Honma R, Sumita M. Cytotoxicity evaluation of 43 metal salts using murine fibroblasts and osteoblastic cells. J Biomed Mater Res. 1998; 39(2): 331–340.

[101] Eto S, Miyamoto H, Shobuike T, et al. Silver oxide-containing hydroxyapatite coating supports osteoblast function and enhances implant anchorage strength in rat femur. J Orthop Res. 2015; 33(9): 1391–1397.

[102] Barthelemi S, Robinet J, Garnotel R, et al. Mechanical forces-induced human osteoblasts differentiation involves MMP-2/MMP-13/MT1-MMP proteolytic cascade. J Cell Biochem. 2012; 113(3): 760–772.

[103] Amar S, Smith L, Fields GB. Matrix metalloproteinase collagenolysis in health and disease. Biochim Biophys Acta Mol Cell Res. 2017; 1864 (11 Pt A): 1940–1951.

[104] Aimes RT, Quigley JP. Matrix metalloproteinase-2 is an interstitial collagenase. Inhibitor-free enzyme catalyzes the cleavage of collagen fibrils and soluble native type I collagen generating the specific 3/4- and 1/4-length fragments. J Biol Chem. 1995; 270(11) :5872–5876.

[105] Fields GB. Interstitial collagen catabolism. *J Biol Chem*. 2013; 288(13): 8785–8793.

[106] Sun B, Sun J, Han X, et al. Immunolocalization of MMP 2, 9 and 13 in prednisolone induced osteoporosis in mice. Histol Histopathol. 2016; 31(6): 647–656.

[107] Jonitz-Heincke A, Lochner K, Schulze C et al. Contribution of human osteoblasts and macrophages to bone matrix degradation and proinflammatory cytokine release after exposure to abrasive endoprosthetic wear particles. Mol Med Rep. 2016 Aug; 14(2): 1491–500.

[108] Xie J, Hou Y, Fu N, et al. Regulation of Extracellular Matrix Remodeling Proteins by Osteoblasts in Titanium Nanoparticle-Induced Aseptic Loosening Model. J Biomed Nanotechnol. 2015; 11(10): 1826–1835.

[109] Laronha H, Carpinteiro I, Portugal J, et al. Challenges in Matrix Metalloproteinases Inhibition. Biomolecules. 2020; 10(5): 717.

[110] Arpino V, Brock M, Gill SE. The role of TIMPs in regulation of extracellular matrix proteolysis. Matrix Biol. 2015; 44–46: 247–254.

[111] Stetler-Stevenson WG. Tissue inhibitors of metalloproteinases in cell signaling: metalloproteinase-independent biological activities. Sci Signal. 2008; 1(27): re6.